Petrides, M. and Zlatkina, V.

Morphological patterns of the postcentral sulcus in the human brain.

Submitted to and accepted by:
Journal of Comparative Neurology, 518(18), 3701-3724.

doi: 10.1002/cne.22418
http://onlinelibrary.wiley.com/journal/10.1002/(ISSN)1096-9861

Zlatkina, V., & Petrides, M. (2010). Morphological patterns of the postcentral sulcus in the human brain. ***Journal of Comparative Neurology*****,** ***518*****(18), 3701-3724.**
DOI: 10.1002/cne.22418

This research was supported by Canadian Institutes of Health Research (CIHR) grant MOP-14620 to M. Petrides.

The morphological structure of the postcentral sulcus and its variability were investigated in 40 structural magnetic resonance images of the human brain registered to the Montreal Neurological Institute (MNI) proportional stereotaxic space. This analysis showed that the postcentral sulcus is not a single sulcus, but rather a complex of sulcal segments separated by gyri which merge its banks at distinct locations. Most of these gyri are submerged deep within the sulcus and can be observed only by examining the depth of the sulcus, although a small proportion may be observed from the surface of the brain. In the majority of the examined cerebral hemispheres (73.75%), the postcentral sulcus is separated into two or three segments, and less frequently into four or five segments (12.5%) or remains continuous (13.75 %). Examination of the in-depth relationship between the postcentral sulcus and the intraparietal sulcus revealed that these two sulci may appear to join on the surface of the brain, but they are in fact always separated by a gyrus in the cortical depth. In 32.5% of the examined hemispheres, a dorso-ventrally oriented sulcus, the transverse postcentral sulcus, is located anterior to the postcentral sulcus on the lower part of the postcentral gyrus. Systematic examination of the morphology of the postcentral sulcus in the proportional stereotaxic space which is used in functional neuroimaging studies is the first step towards the establishment of anatomical-functional correlations in the anterior parietal lobe.

Introduction

The postcentral gyrus, which forms the anterior part of the parietal lobe, is delimited by the central sulcus, anteriorly, and the postcentral sulcus, posteriorly (Figure 1). Pioneer studies using electrical stimulation during brain surgery established that, as in nonhuman primates, the postcentral gyrus of the human brain is the somatosensory cortex and that there is an orderly arrangement of sensory representations of the different parts of the body along its dorsoventral extent (Penfield and Rasmussen, 1952; Woolsey et al., 1979). More recently, the organization of the somatosensory cortex along the postcentral gyrus of the human brain has been examined and confirmed with functional neuroimaging (Nakamura et al., 1998; Boling et al., 1999, 2002; Fabri et al., 2005). The postcentral sulcus, which separates the postcentral gyrus from the posterior parietal cortex, is traditionally described as a prominent sulcus extending from the superior aspect of the hemisphere to the lateral fissure (e.g. Ono et al., 1990; Duvernoy et al., 1991). It is sometimes illustrated as a single continuous sulcus (e.g. Smith, 1907; Economo and Koskinas, 1925) or divided into two or three segments which are superior and inferior to each other (e.g. Eberstaller, 1890; Retzius, 1896; Brodmann, 1909; Sarkissov et al., 1955; Ono et al., 1990). The dorsal end of the postcentral sulcus is often depicted as a V-shaped structure consisting of two branches coming together at one point (Brodmann, 1909; Economo and Koskinas, 1925; Sarkissov et al., 1955). A simple single branch termination of the dorsal postcentral sulcus is less frequently described (Eberstaller, 1890; Smith, 1907; Ono et al., 1990).

Various patterns of how the postcentral sulcus relates to neighbouring sulci have been reported. In some cases, a continuous postcentral sulcus or one of its segments merges with the horizontal intraparietal sulcus (Eberstaller, 1890; Retzius, 1896; Brodmann, 1909; Economo and Koskinas, 1925; Sarkissov et al., 1955; Ono et al., 1990). In other cases, the postcentral sulcus and the intraparietal sulcus appear to be separated by a narrow, often submerged, gyrus (Retzius, 1896; Smith, 1907; Ono et al., 1990). With regard to the cingulate sulcus, when its marginal ramus is visible on the lateral surface of the brain, it is often shown to terminate between the two branches of a bifurcated dorsal end of the postcentral sulcus (Brodmann, 1909; Economo and Koskinas, 1925; Ono et al., 1990).

The existing studies of the morphological variations of the border between the postcentral gyrus (somatosensory cortex) and the posterior superior and inferior parietal lobules, which is formed by the postcentral sulcus, namely the focus of the present investigation, were largely based on visual inspection of the outer cortical surface of post-mortem human brain specimens.

The general features of the sulcal and gyral morphology of this region were established, such as the general location and orientation of the superior and inferior postcentral sulci. However, the limitations of such an approach are evident as shown by the fact that, in a large number of brains, the superior and inferior postcentral sulci may appear to merge superficially with each other and the intraparietal sulcus (i.e. the sulci cannot be differentiated on the outer cortical surface) and yet they may be distinct entities if one were to examine their shape below the surface of the cortex. Similarly, little attention was given in the past to small sulci adjacent to the postcentral sulcus which may have an important role as anatomical/ functional landmarks. Thus, there are limits to how precisely the substantial variability of cortical folding patterns exhibited both between individual human brains and between the two hemispheres of a single brain can be studied with traditional visual inspection. Furthermore, there has been no quantitative examination of these sulci and the patterns they form in a standard stereotaxic space, which is the space within which modern anatomical and functional studies of the human brain are conducted.

The development of neuroimaging technologies at the end of the 20th century provided a new effective methodology for the systematic study of the morphology of the gyri and sulci of the human brain. Appropriate neuroimaging software permits the simultaneous examination of an anatomical feature of interest in several two-dimensional planes, such as coronal, sagittal and horizontal, permitting the accurate charting of the depth and continuity of a particular sulcus from different sections at each point along its length (e.g. Germann et al., 2005). It is particularly important to follow the course of each sulcus from its appearance on the surface of the brain to the fundus because a prominent sulcus which may look continuous on the surface of the brain may be segmented into several major subunits in its depth by submerged gyri that form bridges between the banks of this sulcus (Regis et al., 2005). These bridging gyri have been called “plis de passage” (crossing folds) by Gratiolet or “annectant gyri” by Cunningham and Horsley (Germann et al., 2005; Huttner et al., 2005; Regis et al., 2005). When a specific pli de passage (annectant gyrus) is visible from the surface of the brain, a particular sulcus may be judged by visual inspection as discontinuous and it can be marked as several separate (and sometimes unrelated) sulci on certain anatomical maps, but if the pli de passage is not visible from the surface, the same sulcus may be marked as continuous and its branches not recognized. Moreover, unusual sulcal patterns may originate when segmented portions of the main sulci merge with each other on the cortical surface. Regis et al. (2005) argue that there is a good correspondence between the interruptions of the main sulci described in the literature and the

positions of submerged plis de passage. Thus, it may be possible to classify large inter-individual variability of sulcal structures observed in the human brain into simpler sulcal patterns by considering the basic sulcal subunits in the deepest fundal region (Huttner et al., 2005; Regis et al., 2005).

The importance of the careful study of the local morphological variability of sulci in the human brain was recently highlighted in our laboratory when it was shown that a major controversy could be resolved by examining functional activity in relation to the variations in local sulcal and gyral morphology (Amiez et al., 2006). A frequent approach in functional neuroimaging studies is to average activity observed in a number of subjects in the standard proportional stereotaxic space to determine stereotaxic coordinates of the brain region involved in a specific sensory or motor process. In such cases, any relation of activity in individual subjects to variations in sulcal and gyral morphology is obscured. While this approach does not pose major problems when an approximate location of a functional activity is searched for, functional activities related to two distinct processes but located close to each other cannot be resolved by examination of the average activity peaks. We have shown that examining functional activity in relation to the local sulcal variability can provide important insights into structure/function relations that are impossible when activity is averaged (Amiez et al., 2006). For instance, when the functional activations in dorsal posterior frontal cortex during a visuomotor hand conditional task and a saccadic eye movement task are averaged across brains, the resulting average activation peaks cannot be differentiated, but a subject-by-subject analysis demonstrates separate locations for the two functional peaks and a clear relationship between a specific type of functional activity and the local sulcal morphology (Amiez et al., 2006). Visuomotor hand conditional activity related to the hand premotor cortical region is localized in the dorsal branch of the superior precentral sulcus, while the saccadic eye movement activity occupies the ventral branch of the superior precentral sulcus (Amiez et al., 2006). It is clear, then, that in order to study functional organization of the cerebral cortex in detail, we must be fully aware of the extent to which the sulcal and gyral morphology differs between individual brains, as well as to be able to identify those anatomical patterns which are common among individuals. Systematic examination of the postcentral sulcus in the standard proportional stereotaxic space employed in functional neuroimaging studies is the first step towards establishment of anatomical-functional correlations in the anterior parietal lobe.

The goal of the present study was to examine the morphological variability of the postcentral sulcus by following its course from the surface of the brain to the fundus in magnetic resonance imaging (MRI) scans. The aim was to provide a detailed examination of the morphology and variability in the morphology of the postcentral sulcus in the two hemispheres of the human brain to aid in the investigation of functional activity related to complex somato-motor function since the postcentral sulcus forms the border of the postcentral gyrus (somatosensory cortex) with the anterior parts of both the superior and inferior parietal lobules which are known to play important roles in the control of action, including action related to writing (for review, see Petrides and Pandya, 2002). We consider two types of gyri, submerged in the fundal depth and extending from the fundus to the cortical surface as they separate individual sulcal segments. The aim was to determine the patterns formed by the postcentral sulcus with the rest of sulci in the anterior parietal lobe by considering true connections in the fundal depth. In addition, accessory sulci and their relation to the main postcentral branches, which have not been previously described, are examined so that a complete understanding of the morphology of the postcentral sulcus can emerge. In the present study the postcentral sulcus was examined in MRI brain volumes transformed in the Montreal Neurological Institute (MNI) proportional stereotaxic space (Evans et al., 1992; Mazziotta et al., 1995a,b), which is a further development of the stereotaxic space of Talairach and Tournoux (1988). The standardized proportional stereotaxic space provides a common quantitative framework and it is used for accurate communication, comparison and correlation of specific clinical and experimental data obtained in various neuroimaging studies (Chiavaras et al., 2000).

Materials and methods

Subjects

MRI scans of 40 human brains were randomly selected from the population of brain scans in the International Consortium for Brain Mapping (ICBM) database (Mazziotta et al., 1995a, 1995b). The examined sample consisted of 24 males (mean age 23.4 years, SD 3.18) and 16 females (mean age 24.6 years, SD 4.33). All subjects were right-handed, had a negative history of neurological and/or psychiatric disorders, and gave informed consent.

Magnetic Resonance Imaging

All MRI scans were performed on a Philips Gyroscan 1.5T superconducting magnet system. By means of a fast-field echo 3-D acquisition sequence, 160 contiguous 1-mm T_1-weghted images (T_r = 18 msec, T_e = 10 msec, flip angle 30 degrees) were collected in the sagittal plane. Each acquired MRI volume was transformed into the MNI standard proportional stereotaxic space using an automated registration program with a three-dimensional (3D) cross-correlation approach to match the single MRI volume with the intensity average of 305 brain volumes previously aligned into standardized stereotaxic space (Evans et al., 1992; Collins et al., 1994). This transformation was necessary to normalize and correct the MR images for interindividual differences in gross brain size. The transformed brain volumes were then re-sampled on a 1-mm^3 isotropic grid (1mm x 1mm x 1mm voxel size). The thickness of obtained coronal, sagittal and horizontal slices was 1 mm.

The anterior commissure serves as the origin of the MNI stereotaxic space (x = 0, y = 0, z = 0) where the coordinates are given in millimetres. The medio-lateral (left-right) axis is represented by the x coordinate (positive values represent the right hemisphere), the rostro-caudal (anterior-posterior) axis by the y coordinate (positive values are rostral to the anterior commissure), and the dorso-ventral (superior-inferior) axis by the z coordinate (positive values are superior to a horizontal line drawn through the anterior and posterior commissures).

Segmentation of intrasulcal gray matter

An interactive 3D imaging software package DISPLAY (MacDonald, 1996) was used to mark the parietal sulci on individual MRI brain scans. DISPLAY allows the scans to be viewed simultaneously in the coronal, horizontal and sagittal planes of section. When the cursor, controlled by the mouse, was moved to any location in a given section, the sections in the other two planes were automatically updated to show the corresponding views of the location of interest. The movement of the cursor was also observed on a 3-D reconstruction of the brain surface.

The overall intensity of sections and gray-white matter contrast were adjusted in DISPLAY, so that each sulcus could be clearly observed from the surface of the brain to its fundus. The cerebrospinal fluid voxels between the banks of individual sulci were manually selected by ‘coloring’ them with the ‘mouse-brush’ tool. Each sulcus of interest was identified using a specific color label to mark the space within its banks along its entire course. The sulci of

interest were examined in 1-mm steps in all planes of section to determine their direction and extent, as well as to establish at which point they terminate i.e. they may no longer be observed in either one of three corresponding slices.

Surface renderings

Three-dimensional surface renderings of individual brains were acquired using two different types of software. Initially, an automatic, model-based, surface deformation algorithm was used to reconstruct 40 brain volumes already existing in the MNI stereotaxic space into three-dimensional objects and visualize the labelled sulci on the outer surface of individual volumes (MacDonald et al., 1994). After the sulcal labels were marked on contiguous two-dimensional sections (coronal, horizontal and sagittal), they were projected to and viewed on the three-dimensional reconstructions of 40 MRI brain volumes. In addition, Caret v.5.5 software was used to reconstruct the same 40 MRI brain volumes placed in the MNI space in three dimensions and slightly 'inflate' them to reveal the deep or submerged parts of sulci, not commonly seen from the surface of the brain (Van Essen, 2005). Such slight "inflation" retained the characteristic shape of the sulci of a given brain volume but allowed inspection of their depth.

After 40 structural MRI brain volumes were imported into Caret 5.5, they were up-registered to the Washington University stereotaxic coordinate space 711-2B-111, which is a version of the Talairach stereotaxic space with an origin at the anterior commissure (Van Essen, 2005). Following registration, the brain volumes were re-sampled on an isotropic grid with 1-mm^3 voxel size. Volume segmentation and initial surface reconstruction were done using SureFit algorithm, which is a part of Caret 5.5 software. Topological errors produced during segmentation were corrected using an automated processing sequence and manual editing in order to remove various irregularities. A segmentation boundary created using SureFit processing sequence was approximately equidistant from the inner and outer limits of the cortical gray matter (cortical layer 4). Initial 'raw' surface generated along the segmentation boundary was 'smoothed' to produce a 'fiducial" surface which is an improved representation of the 3D cortical surface. The quality of cortical segmentation produced with Caret 5.5 was evaluated by visual examination of the generated 3D surfaces and their comparison with the 3D renderings created using an automated algorithm developed by MacDonald and colleagues (1994). Three-dimensional surface reconstructions of 40 brain volumes generated with two different types of

software showed the same external surface features of sulcal and gyral morphology in corresponding volumes. In the final step Caret 5.5 software was used to inflate the surface of brain volumes using up to two smoothing iterations and an inflation factor equal to 1.02. This operation created an effect of opening up the sulci of interest and revealing the submerged parts of sulcal anatomy. Slightly inflated 3D surface reconstructions produced with Caret 5.5 were used to emulate the external surface view of postmortem brains. The procedure for segmentation of T1-weighted structural MRI volumes is described in detail in "Caret 5 Tutorial: segmentation, flattening and registration" available from Van Essen Lab Wiki Home Page (http://brainvis.wustl.edu).

Stereotaxic coordinates of the submerged gyri (submerged plis de passage) of the postcentral sulcus

Stereotaxic coordinates of the midpoints (centers) of the submerged gyri of the postcentral sulcus were determined manually on horizontal sections of the MRI brain volumes. All horizontal sections belonging to a volume were examined at 1 mm intervals. When a section which contained two segments of the postcentral sulcus separated by a submerged gyrus was encountered, it was examined to determine whether one of the segments of the postcentral sulcus was at its deepest and most ventral fundal point i.e. no sections ventral to the current section contained the same sulcal segment. Once the section of interest was found, the stereotaxic coordinates of the central point of the submerged gyrus between the two segments were determined manually. Given the small size of submerged gyri in the examined sections, the error in determining their central point is expected to be less than 2-3 mm in the anterior-posterior (y) and medial-lateral (x) axes. There is little to no error in the dorso-ventral (z) coordinate of the midpoints of submerged gyri because the midpoints were determined in the sections containing the deepest fundal regions of sulcal segments and the sulcal segments were not observed in the sections immediately ventral to the sections of interest. Although the current values of the stereotaxic coordinates of four submerged gyri are estimates of their actual central points, the estimated coordinates always fall within the larger regions of the submerged gyri and therefore are still indicative of their location.

Results

Postcentral sulcus

The present examination of the postcentral sulcus in 80 hemispheres of human MRI brain scans revealed that the postcentral sulcus can either remain continuous or it may be separated into segments by gyri, which merge its banks. Some of the gyri, which divide the postcentral sulcus into segments, may be visible from the surface of the brain, while others are hidden deep within the sulcus (submerged gyri; Figures 2-10). Submerged gyri separate the postcentral sulcus into segments by merging its banks at specific locations close to the fundus. Submerged gyri can be identified only in serial sections. Gyri visible from the surface of the brain, i.e. non-submerged gyri, merge two banks of the postcentral sulcus both in depth and on the surface. They are identified equally well on three-dimensional reconstructions of MRI brain volumes and cross-sections.

In the present paper, submerged gyri are called submerged plis de passage and non-submerged gyri are called visible gyri. Additionally, terms submerged plis de passage and visible gyri are combined under a more broad term interrupting gyri, i.e. gyri which divide the postcentral sulcus into segments.

In some hemispheres both types of interrupting gyri were present, submerged plis de passage and visible gyri (17.5% of all hemispheres). In the majority of hemispheres only one type of interrupting gyri was present, either submerged plis de passage (42.5% of hemispheres) or visible gyri (26.25% of hemispheres). In the rest of hemispheres (13.75%), no interrupting gyri could be identified.

The results show that the postcentral sulcus can be divided into five segments by four submerged plis de passage and/or visible gyri. In the majority of examined brains, the postcentral sulcus contained less than five segments and less than four interrupting gyri were observed in each individual hemisphere.

The postcentral sulcus was continuous and could be followed without any interruption from its dorsal end to the ventral end in 13.75% of all hemispheres (see Table 1). Most frequently, however, the postcentral sulcus consisted of either 2 segments (46.25% of all hemispheres) or 3 segments (27.5% of all hemispheres). In a small number of cases, the postcentral sulcus contained 4 to 5 segments (Table 1).

The averaged estimates of the stereotaxic coordinates were established for four submerged plis de passage, described as the first, second, third and fourth submerged plis de

passage (see Methods; Table 2). The first submerged pli de passage is most dorsal and the fourth submerged pli de passage is most ventral with respect to the rest of submerged plis de passage.

The stereotaxic coordinates could not be found for the visible gyri because of their relatively large size and continuity. However, in the MNI stereotaxic space, the locations of four visible gyri were found to correspond generally to locations of four submerged plis de passage. Therefore, in order to describe spatial location of a visible gyrus a reference will be made to a specific submerged pli de passage, whose estimated stereotaxic coordinates fall within the cortical region occupied by the visible gyrus.

In 47.5% of all examined hemispheres both types of interrupting gyri, i.e. submerged plis de passage and visible gyri, occurred at the stereotaxic location of the third submerged pli de passage. Interrupting gyri at the location of the first, second and fourth submerged plis de passage were observed in 37.5%, 22.5% and 25% of all hemispheres respectively (see Table 3 and Figure 2).

The majority of gyri located at the stereotaxic location of the third and fourth submerged plis de passage in the left and right hemispheres were submerged gyri, whereas most of the gyri located next to the first submerged pli de passage were visible on the surface of the brain (see Table 3).

Both submerged plis de passage and visible gyri were more frequently found in the left hemisphere than in the right hemisphere.

Hemisphere differences

There were hemispheric differences in the segmentation of the postcentral sulcus in the forty MRI brain volumes examined (see Table 1). On average, in the right hemisphere, the postcentral sulcus consisted of fewer segments than in the left hemisphere. More specifically, the postcentral sulcus was continuous or consisted of two segments in a larger number of right hemispheres (72.5%) than left hemispheres (47.5%). The postcentral sulcus consisting of three, four and five segments was located more often in the left hemisphere (52.5%) than the right hemisphere (27.5%). The left hemisphere contained more interrupting gyri at the stereotaxic coordinates of the first, third and fourth submerged plis de passage (see Table 3). Interrupting gyri at the location of the second submerged pli de passage were distributed approximately equally between the left and right hemispheres.

Segmentation patterns comparison between two hemispheres of individual brains

When two hemispheres of the same brain were compared to each other with regard to the number of segments of the postcentral sulcus, it was observed that in approximately one fourth of all brains (27.5% or 11 brains) the postcentral sulcus showed the same type of segmentation. In 15% of all brains both hemispheres contained the postcentral sulcus consisting of two segments and in 10% of the brains the postcentral sulcus was divided into 3 segments in both hemispheres of the same brain.

In 55% of the brains (22 brains) the postcentral sulcus showed a certain number of segments in one hemisphere and had this number increased by one (i.e. contained one extra segment or +1 pattern) in the other hemisphere of the same brain. For instance, the postcentral sulcus contained 2 segments in the right hemisphere and 3 segments in the left hemisphere. The majority of brains demonstrated a less segmented pattern in the right hemisphere and a more segmented +1 pattern in the left hemisphere.

In 17.5% of the brains (7 brains) the postcentral sulcus showed +2, +3 or +4 levels of segmentation in the opposite hemisphere. As an example, the postcentral sulcus consisted of 2 segments in the right hemisphere and 4 segments in the left hemisphere. Alternatively, the postcentral sulcus could be continuous in the right hemisphere and contain 3, 4 or 5 segments in the left hemisphere. In these cases, the left hemisphere was always associated with a more segmented postcentral sulcus and the right hemisphere with a less segmented postcentral sulcus.

Surface view vs. cross-section view

In order to characterize the postcentral sulcus and its segments earlier investigators frequently used visual observation of the external brain surface, which contained sulci and non-submerged (visible) gyri. As a result, the postcentral sulcus was often described as a continuous sulcus or a set of two to three sulci which cross the brain surface in a dorso-ventral direction. The present investigation, which considers the postcentral sulcus in its depth, suggests that the postcentral sulcus may consist of up to five segments separated by submerged and non-submerged gyri.

In order to see how two methodologies compare, we applied both methods to the same population of 40 human MRI brain volumes. First, we identified and followed the postcentral sulcus and its segments in horizontal, sagittal and coronal sections. Next, we identified and described the postcentral sulcus in 3D Caret reconstructions of the same brain volumes. The results were compared with each other. In only 25% of cases when the postcentral sulcus was

characterized as continuous using surface-based methodology, was it also described as continuous when using cross sections to examine the depth (Figure 2a). In 57% of hemispheres where the postcentral sulcus was determined to consist of 2 segments using surface-based methodology, it was also determined to contain 2 sulcal segments by means of cross section analysis (Figures 2b, 3-6). In the remaining 43% of hemispheres described as containing the postcentral sulcus with 2 segments through surface observation, the postcentral sulcus was found to consist of three to five segments in cross sections (Figure 2e). Using surface-based methodology, the postcentral sulcus was found to consist of 3 segments in only 6% of all hemispheres (Figure 2d), whereas cross-section analysis found that 27.5% of all hemispheres contained the postcentral sulcus with three segments. Only cross-section analysis and not the surface-based descriptions of the postcentral sulcus found that it may consist of four to five sulcal segments. Therefore, although there is a partial overlap between results obtained with 2 different methods, the surface-based analysis can not be used as an accurate predictor of submerged morphology of the postcentral sulcus.

Dorsal end of the postcentral sulcus

Analysis of the postcentral sulcus in horizontal sections revealed that the most frequent type of dorsal termination of the sulcus was bifurcation (68.75% of all hemispheres) followed by a standard straight line (23.75%; see Table 4 and Figure 11). Least often the postcentral sulcus terminated with 3 short extensions or branches (7.5%; Figure 11e). Comparison between two hemispheres showed that bifurcation of the dorsal end more often occurred in the left hemisphere, while a straight line end was more common in the right hemisphere (see Table 4).

Patterns of the postcentral sulcus

Connection with the lateral fissure

Surface observation of the postcentral sulcus shows that, in some brains, it appears to merge with the lateral fissure i.e. the separating gyrus between the two sulci is too small to be detected visually. We identified a similar pattern in 3D surface reconstructions of 40 MRI brain volumes and correlated it with the number of segments of the postcentral sulcus, which were determined using cross-section analysis. Our findings show in a third of all hemispheres (30%) the postcentral sulcus forms a superficial connection with the lateral fissure (see Table 5 and Figure 11a,c). Additionally, the greater the number of segments the postcentral sulcus has, the

more often it seems to merge with the lateral fissure in 3D reconstructed images. Thus, in 62.5% of all hemispheres with 4 segments of the postcentral sulcus, 43.5% of hemispheres with 3 segments of the postcentral sulcus, and 21.6% of all hemispheres with 2 segments of the postcentral sulcus, the postcentral sulcus appeared to merge with the lateral fissure. In contrast, only 9% of hemispheres with the continuous postcentral sulcus showed a surface connection with the lateral fissure.

As analyzed with the surface-based and cross-section methodology, a larger proportion of brains in which the postcentral sulcus seemed to merge with the lateral fissure contained a bifurcated dorsal termination of the postcentral sulcus (36.4%) as opposed to a regular straight line termination (21.1%).

Same brain differences with regards to the postcentral sulcus connection with the lateral fissure

The results show that when the postcentral sulcus does not appear to merge with the lateral fissure in one hemisphere of the brain, then it does not form a superficial connection with the lateral fissure in the other hemisphere in 71.4% of all brains. Conversely, when the postcentral sulcus merges with the lateral fissure in one hemisphere of the brain, then it merges with the lateral fissure in the other hemisphere in only 33% of all brains. In other words, when the postcentral sulcus appears to merge with the lateral fissure in one hemisphere, it is two times more likely not to merge with the lateral fissure in the other hemisphere.

Connection with the superior longitudinal fissure

In approximately one third of all hemispheres (28.75%) the postcentral sulcus reached the superior longitudinal fissure (see Table 4 and Figure 11b,d). However, it did not extend to the medial surface, but remained on the lateral surface very close to the superior longitudinal fissure. There were no differences between the left and right hemispheres with regards to this pattern (see Table 4).

Connection with the intraparietal sulcus

The intraparietal sulcus, also identified as the horizontal segment of the intraparietal sulcus, is located posterior to the postcentral sulcus and it has a more or less horizontal or anterior-posterior orientation. Examination of the intraparietal sulcus both in 3D surface

reconstructions of brain volumes and cross sections showed that the anterior end of the intraparietal sulcus is located at the same dorso-ventral level as the superior frontal sulcus.

External surface-based analysis of the connection between the postcentral sulcal complex and the anterior part of the intraparietal sulcus in 40 reconstructed MRI brain volumes showed that the anterior intraparietal sulcus was separated from all segments of the postcentral sulcus simultaneously by a visible (non-submerged) gyrus in 40% of all hemispheres (see Table 6 and Figure 12). Less frequently the anterior intraparietal sulcus was determined to merge superficially with the continuous postcentral sulcus (31.25% of all hemispheres). In 20 % of all hemispheres the intraparietal sulcus connected superficially with the inferior segment of the postcentral sulcus and it was separated by a visible gyrus from the superior segment of the postcentral sulcus. In a small number of cases the anterior intraparietal sulcus appeared to merge with the superior (6.25% of all hemispheres) or middle (2.5% of all hemispheres) segment of the postcentral sulcus and it was separated by a gyrus from the rest of the segments of the postcentral sulcal complex (see Table 6 and Figure 12).

Anterior intraparietal sulcus appeared to merge with the middle or inferior postcentral sulcus more often in the left hemisphere than in the right hemisphere, while it connected superficially with the superior segment of the postcentral sulcus mainly in the right hemisphere (see Table 6).

Investigation of the connection between the anterior intraparietal sulcus and the postcentral sulcal complex (which included all postcentral sulcal segments) in horizontal sections showed that the two sulci are always separated by a submerged or visible gyrus (100% of all cases). Therefore, in spite of the superficial connection, the intraparietal and postcentral sulci always have separate origins.

Patterns with the ascending/ marginal branch of the cingulate sulcus

Analysis of the ascending branch of the cingulate sulcus in cross sections showed that it terminated anterior to or between the two branches of a bifurcated (“V”) dorsal end of the postcentral sulcus in the majority of cases (71.25% of hemispheres; see Table 7). Less common was a termination posterior to the dorsal end of the postcentral sulcus (28.75% of hemispheres). Figure 13 shows examples of patterns formed by the ascending branch of the cingulate sulcus and the dorsal termination of the postcentral sulcus.

The ascending branch of the cingulate sulcus terminated anterior to or between the branches of a bifurcated dorsal termination of the postcentral sulcus in a larger number of left than right hemispheres (see Table 7). At the same time, termination posterior to the dorsal end of the postcentral sulcus was more common for the right hemispheres.

Surface-based analysis showed that in 41.25% of all hemispheres the ascending branch of the cingulate sulcus extended to and could be clearly seen on the lateral surface of 3D reconstructions of human brain volumes. This pattern occurred more frequently in the left hemisphere than in the right hemisphere.

Sulci dorsal to the postcentral sulcus

The results of cross-section and surface-based analyses revealed a frequent occurrence of sulci located directly dorsal to the postcentral sulcus. These sulci could be classified into two categories: i) short sulci which remained on the lateral surface of the brain and occurred in approximately one tenth of all hemispheres (11.25%), and ii) somewhat longer sulci which extended to the medial surface of the brain by crossing the superior longitudinal fissure in about one third of all hemispheres (33.75%; see Table 8). Two types of sulci are illustrated in a diagrammatic form in Figure 14.

Both types of sulci were usually located superior to the first submerged pli de passage and they had a horizontal (anterior-posterior) or diagonal orientation. The non-vertical (i.e. or non-dorso-ventral) orientation of the dorsal sulci and their superior position on the lateral surface were the main reasons why the dorsal sulci were not considered to be segments of the postcentral sulcus.

Dorsal sulci which extended to the medial surface of the brain (type ii) were more often observed in the left hemisphere, while the sulci which remained on the lateral surface and did not extend to the medial surface (type i) were more commonly found in the right hemisphere (see Table 8).

Analysis of two hemispheres of the same brain showed that when one hemisphere of the brain contained sulci which were located dorsal to the postcentral sulcus and extended to the medial surface (type ii), then there was a 22% chance that the opposite hemisphere of the same brain would also contain comparable sulci. The probability to find similarly placed sulci in the opposite hemisphere of the same brain was smaller (11%) for the dorsal sulci which remained on the lateral surface and did not extend to the medial surface (type i). Therefore, in the majority of

brains, only one hemisphere contained sulci which were located directly dorsal to the postcentral sulcus.

It seems possible that in some specimen the postcentral sulcus joins with the sulci located dorsal to it at the level of their fundus deep inside the brain, such that the individual origins of sulci cannot be detected in cross sections. In this case, the postcentral sulcus would be considered to extend to the dorso-medial edge of the hemisphere and make a connection with the superior longitudinal fissure.

Sulcal patterns on the inferior postcentral gyrus

In this paper a portion of the postcentral gyrus located ventral to the second submerged pli de passage of the postcentral sulcus is referred to as the inferior postcentral gyrus. In 45% of all hemispheres, there were no sulci located on the inferior postcentral gyrus (see Table 9). In one third of all hemispheres (32.5%) we observed a sulcus of variable length which was located anterior to the postcentral sulcus on the inferior postcentral gyrus (Figure 15). It had a vertical dorso-ventral orientation and it was often placed in parallel with the postcentral sulcus (Figure 15). This sulcus was named the transverse postcentral sulcus.

Occasionally, the transverse postcentral sulcus could appear to connect with the lateral fissure on the surface of reconstructed 3D brain volumes, but cross-section analysis confirmed that the transverse postcentral sulcus was always separated from the lateral fissure by a gyrus. The length of the transverse postcentral sulcus varied from brain to brain. The transverse postcentral sulcus was most often seen in combination with the postcentral sulcus which contained 2 segments (50%) and less often with the continuous postcentral sulcus (27%) or the postcentral sulcus consisting of 3 segments (19%; also Figure 15).

As verified with the surface-based analysis, the transverse postcentral sulcus was present in hemispheres where the postcentral sulcus did not merge superficially with the lateral fissure (96.2%). The transverse postcentral sulcus was more often present in the right hemisphere of the brain (61.5%) than in the left hemisphere (38.5%; see Table 9).

Averaged data show that in the hemispheres where the transverse postcentral sulcus was absent, the postcentral sulcus terminated ventral to the fourth submerged pli de passage. In the hemispheres with the transverse postcentral sulcus, the postcentral sulcus terminated close to the stereotaxic coordinates corresponding to the third submerged pli de passage, while the transverse postcentral sulcus started at the stereotaxic location of the second submerged pli de passage.

We suggest that the transverse postcentral sulcus belongs to the postcentral sulcal complex and it may be considered an inferior part of the postcentral sulcus on the basis of the following evidence: i) the transverse postcentral sulcus appears around the base of the second submerged pli de passage in horizontal sections; ii) the transverse postcentral sulcus is mostly present when the postcentral sulcus consists of 2 segments; iii) the transverse postcentral sulcus is located anterior to the postcentral sulcus and it often overlaps with the ventral end of the postcentral sulcus; iv) the transverse postcentral sulcus is present in the brains with a shorter length of the postcentral sulcus and does not appear in the brains where the postcentral sulcus merges superficially with the lateral fissure.

It is possible that in some of the brains examined in the present study the transverse postcentral sulcus merged with the postcentral sulcus in the fundus and it did not appear as an independent sulcus anterior to the postcentral sulcus. In those brains the transverse postcentral sulcus was likely to be identified as an integral part of the postcentral sulcus.

In addition to the transverse postcentral sulcus, there were other types of sulci which were observed on the inferior postcentral gyrus. In 53.5% of all hemispheres, sulci which originated on the upper lip of the lateral fissure also extended onto the lateral surface of the brain (e.g. posterior subcentral sulcus, sulcus transverses operculi parietalis primus and secondus, using terminology of Economo and Koskinas, 1925; see Table 9 and Figures 3-10, 11b,d). These sulci appeared as branches of the lateral fissure in 3D surface reconstructions of MRI brain volumes. Sulci from the parietal operculum were much more frequently observed on the inferior postcentral gyrus in the left hemisphere of the brain than in the right hemisphere.

Examples of sulcal features and patterns in two MRI brain volumes

A number of features and patterns of the postcentral sulcus are demonstrated in two hemispheres taken from two different brains within the sample of MRI brain volumes used in this study. Figures 3-6 show cross sections taken from the left hemisphere of an MRI brain volume (case 1). The postcentral sulcus consists of 2 segments which are separated at the first submerged pli de passage by a visible/ non-submerged gyrus (Figures 4c-e, 5i). Both surface-based and cross-section analyses show the same segmentation pattern of the postcentral sulcus. The postcentral sulcus does not form a superficial connection with the lateral fissure (Figure 6l-m). It does not reach the superior longitudinal fissure either. The dorsal termination of the postcentral sulcus is a bifurcation and it has a V- shape (Figure 4a-c). There are no sulci located

dorsal to the postcentral sulcus. The ascending branch of the cingulate sulcus is seen on the lateral surface of the brain (Figures 3, 5l-m; also see the same hemisphere on Figure 2b). It terminates inside the V-end/ bifurcation of the postcentral sulcus (see Figure 4a-c). Surface-based analysis shows that the intraparietal sulcus merges with the inferior segment of the postcentral sulcus (in addition to Figure 3 see Figure 2b). Cross-section analysis shows a submerged gyrus between the intraparietal sulcus and the postcentral sulcus (Figure 4i-j). The transverse postcentral sulcus is located anterior to the postcentral sulcus on the inferior postcentral gyrus and its origin is close to the second submerged pli de passage (see Figures 4g-p, 5a-f, 6k-m). There are no other sulci on the inferior postcentral gyrus.

Figures 7-10 show a number of features of the postcentral sulcus in serial sections taken from the right hemisphere of an MRI brain volume (case 2). On the 3D surface of the brain the postcentral sulcus appears as a continuous sulcus. Analysis of the postcentral sulcus in cross sections reveals that it consists of 3 segments (superior, middle and inferior) separated by the third and fourth submerged plis de passage (Figures 8i-k, 10g, 10l-o). The postcentral sulcus forms a superficial connection with the lateral fissure (Figure 10m-o) and it reaches the superior longitudinal fissure (Figures 8a-b, 9k-o). Dorsal end of the postcentral sulcus is bifurcated and the ascending branch of the cingulate sulcus terminates inside the bifurcation (Figure 8c-e). There are sulci located directly dorsal to the postcentral sulcus, which cross the superior margin of hemisphere (Figure 8b-d). The postcentral sulcus does not merge with the intraparietal sulcus (Figure 8i). There are no sulci on the inferior postcentral gyrus.

Discussion

The present investigation established that the postcentral sulcus is a complex of sulcal segments located directly posterior to the central sulcus, extending from the dorsal aspect of the hemisphere close to the midline to the lateral fissure. The postcentral sulcus was examined systematically in two-dimensional serial sections of 40 MRI brain volumes in the MNI stereotaxic space. This approach permitted us to characterize the submerged structure of the postcentral sulcus and describe in-depth relationships between the postcentral sulcus and its neighboring sulci. It should be noted that the patterns formed by the main sulci deep within the fundus are less variable among individuals than the appearance of sulci on the surface of the brain and the sulcal variability increases, in general, towards the outer cortical surface (Lohmann and Cramon, 2000; Regis et al., 2005). In addition, the presence of submerged gyri within

individual sulci can partition the sulci into basic sulcal units and clarify sulcal patterns on the external cortical surface (Huttner et al., 2005; Regis et al., 2005). The present results show that, in the majority of hemispheres, the postcentral sulcus is separated into two (46.25%) or three (27.50%) segments by gyri that join its banks (Figure 2; Table 1). Less frequently, the postcentral sulcus consists of four or five segments (12.5%) or remains continuous (13.75%). The majority of gyri which divide the postcentral sulcus into segments are submerged deep within the sulcus (submerged plis de passage) and can be observed only in brain sections, while a smaller proportion of gyri may be seen from the surface of the brain (visible gyri; see Table 3). Submerged plis de passage and visible gyri occur in four distinct locations of the MNI stereotaxic space and the locations of the corresponding submerged plis de passage and visible gyri overlap (Table 2).

Cunningham (1892) describes deep annectant gyri which divide the superior and inferior segments of the postcentral sulcus into smaller units. These basic sulcal units appear as small depressions in the fetal brain and unite into larger structures as the brain continues its prenatal and postnatal development (Connolly, 1950). Cunningham's deep annectant gyri are akin to the submerged gyri described in the current study. It may be suggested, that the four submerged plis de passage (submerged gyri) separate five original postcentral sulcal units which appear early in the development of the fetal brain and have specific functional relevance (see below). Cunningham (1892) also mentions the common occurrence of a deep gyrus (the anterior deep annectant gyrus of Eberstaller) which marks the separation between the horizontal segment of the intraparietal sulcus and the inferior postcentral sulcus. This is consistent with the findings of the current study which demonstrated that the postcentral and intraparietal sulci can appear to join on the surface of the brain, but they are in fact always separated by a gyrus in the cortical depth (Figure 4i-j).

Several studies suggest that there may be a relationship between the development of cortical convolutions and the architectonic, functional, and connectional specialization of cortical regions (Connolly, 1950; Welker, 1990; Toro and Burnod, 2005). The position of the main sulci is thought to reflect the underlying cortical organization and be a result of interactions between genetic factors, cytoarchitectonic differentiation, mechanical tension produced by the thalamo-cortical and cortico-cortical fibers, modulatory influence of the afferent fibers on cortical growth, and the initial geometry of the cortex and its asymmetries (Connolly, 1950; Welker, 1990; Van Essen, 1997; Toro and Burnod, 2005). Despite considerable inter-individual variability in sulcal

and gyral morphology, the main sulci demonstrate relatively constant topographical relationships with each other. Although there may not be a simple correspondence between the cytoarchitectonic boundaries and the sulcal fundi (Geyer et al., 1999), structural components of individual sulci (fundus, walls) and gyri (crown, banks) can serve as landmarks which identify the approximate locations of specific architectonic areas in MRI images or real-life brain specimens. At present, accurate borders of cytoarchitectonic areas can be determined only under light microscopy in histological brain sections and not in the MRI images. To address this problem, probability maps reflecting the variability of cytoarchitectonic areas in the standard stereotaxic space have been created for several cortical areas (Geyer et al., 2000; Grefkes et al., 2001; Eickhoff et al., 2006). The probability maps can be used with individual MRI brain volumes to assess the location of functional activations with respect to the averaged locations of cytoarchitectonic areas.

Influential cytoarchitectonic maps subdivided the anterior parietal lobe into several cortical areas. According to Brodmann (1909), the postcentral gyrus may be parcellated into three main architectonic areas: area 3 (the rostral postcentral area which occupies the posterior bank of the central sulcus), area 1 (the intermediate postcentral area which is located on the anterior lip of the postcentral gyrus), and area 2 (the caudal postcentral area that occupies the posterior part of the postcentral gyrus and which extends into the anterior bank of the postcentral sulcus). Brodmann (1909) also pointed out that the granular cortex on the posterior bank of the central sulcus is separated from the agranular motor cortex on the anterior bank of this sulcus by a narrow transitional area in its fundus that has the characteristics of both the agranular and granular areas. Later on, this transitional zone was named area 3a, and Brodmann's area 3 was now referred to as area 3b (Kaas, 1983; Geyer et al., 1999). The cytoarchitectonic map of Sarkissov and colleagues (1955) also shows areas 3, 1 and 2. Economo and Koskinas (1925) provided detailed descriptions of the features of the cytoarchitectonic areas of the postcentral region and corresponding high quality photographic images. The following main areas and their subdivisions were identified in the anterior parietal lobe: PA (PA_1, PA_2), PB (PB_1, PB_2), PC and PD. Area PA_1 (which corresponds to area 3a of Brodmann) occupies the fundus and the lowermost part of the posterior wall of the central sulcus. It extends from the ventral end of the central sulcus, where it can be seen slightly on the lateral surface of the brain to the dorsal end of the central sulcus and the surrounding region on the medial surface of the brain (Economo, 2009). Area PA_2 follows the ascending branch of the cingulate sulcus from the paracentral lobule

to the dorsal-posterior part of the postcentral gyrus and the superior parietal lobule (Economo, 2009). On the lateral surface of the brain area PA_2 is located posterior to the dorsal extent of area PC. Economo and Koskinas' area PB occupies the upper two-thirds of the posterior wall of the central sulcus and extends in parallel to area PA_1 from the ventral end of the central sulcus to its dorsal end on the paracentral lobule. Subdivisions PB_1 and PB_2 reflect inhomogeneity in granularity within area PB; they form strips and islets throughout this area. Area PB corresponds to area 3 of Brodmann that subsequently came to be referred to as area 3b in order to distinguish it from the transitional zone, area 3a. Area PC forms a wide strip posterior to area PB (Economo and Koskinas, 1925) and occupies the visible part of the postcentral gyrus (the crown and the lips) and it extends from the parietal operculum to the paracentral lobule. Area PC may correspond, in part, to areas 1 and 2 of Brodmann. Area PD of Economo and Koskinas occupies the walls and the fundus of the postcentral sulcus along its entire length (Economo, 2009). A recent investigation examined the extent of Brodmann area 2 in 10 post-mortem human brains using two types of analysis, observer-dependent (analysis of histological sections under the light microscope) and observer-independent (analysis of histological sections using a computer algorithm) (Grefkes et al., 2001). The findings showed that area 2 was always located within the anterior wall of the postcentral sulcus and the position of its borders varied between the individual brains (Grefkes et al., 2001). The anterior boundary of area 2 could reach the crown of the postcentral gyrus and the posterior boundary could extend slightly caudal to the fundus of the postcentral sulcus. The dorsal and ventral boundaries of area 2 were located within several millimeters of the dorsal and ventral terminations of the postcentral sulcus. In the brains with the segmented postcentral sulcus, area 2 traversed the dividing gyral bridges without any interruptions in its continuity (Grefkes et al., 2001).

The present results demonstrate that, in approximately two thirds of the examined hemispheres, the postcentral sulcus has a bifurcated dorsal termination, which resembles the shape of the letters Y and V (Table 4). In the rest of the hemispheres, the postcentral sulcus has a single dorsal ending similar to the letter I (see Figures 11 and 13; Table 4). The architectonic maps of Brodmann (1909), Economo and Koskinas (1925) and Vogt (1911) show an architectonically distinct area located between the branches of the dorsal termination of the postcentral sulcus and extending onto the medial surface of the brain (area 5 of Brodmann, 1909; area PA_2 of Economo and Koskinas, 1925; area 75 of Vogt, 1911). In the study by Scheperjans et al. (2005) Brodmann area 5 was found to consist of one lateral (5L) and two medial (5M and

5Ci) subareas. The lateral subdivision of area 5 (5L) was located within the dorsal end of the postcentral sulcus near the superior longitudinal fissure. Area 5L extended from the anterior wall to the posterior wall of the dorsal termination of the postcentral sulcus or approached the ascending branch of the cingulate sulcus on the lateral surface of the brain. Area 5L was located posterior and medial to area 2 and it replaced area 2 in the anterior wall of the dorsal end of the postcentral sulcus (Scheperjans et al., 2005). The most dorsal part of lateral area 5 could be observed occasionally on the cortical surface of neighboring gyri, including the crown of the postcentral gyrus or between the branches of the postcentral sulcus. In the monkey, area 5 receives proprioceptive information from the postcentral somatosensory cortex and appears to play an important role in the encoding of arm postures and movement in space within a body-centered reference frame. It is believed to participate in the coordinate transformation and sensorimotor guidance of motor behavior (Kalaska, 1996; Wenderoth et al., 2004). Neuroimaging research on human subjects implicates area 5 in the performance of directional goal-directed hand movements under somatosensory control (Wenderoth et al., 2004) and performance of movements under proprioceptive control without visual feedback (Grefkes et al., 2004). Stereotaxic coordinates of functional activations localized in putative Brodmann area 5 in the above neuroimaging studies are x = -26, y = -36, z = 74 (Grefkes et al., 2004) and x = -12, y = -50, z = 70; x = 18, y = -46, z = 74; and x = 20, y = -46, z = 72 (Wenderoth et al., 2004). These coordinates tend to place area 5 activations close to the point of bifurcation of the dorsal end of the postcentral sulcus, adjacent to the dorsalmost end of the single dorsal termination of the postcentral sulcus and dorsal to both of these structures, as established in the present study in the MNI stereotaxic space.

Neurophysiological work on non-human primates discovered a set of areas located along the intraparietal sulcus. Of particular interest for the present investigation is the most anterior of these areas, the anterior intraparietal area (AIP), which is located in the anterior part of the lateral bank of the intraparietal sulcus in the monkey brain (Gallese et al., 1994; Sakata et al., 1995). In the monkey, AIP is involved in grasping movements, which depend on the shape of an object to be manipulated (Gallese et al., 1994; Sakata et al., 1995; Baumann et al., 2009). In the human, the presumed homologue of AIP is activated by visual and tactile tasks, which involve three-dimensional attributes of objects, such as shape, size and orientation (Binkofski et al., 1998; Grefkes et al., 2002; Frey et al., 2005; Zhang et al., 2005). Based on the currently available, yet limited knowledge of the anatomo-functional organization of the intraparietal sulcus in the

human, the following two possibilities can be entertained regarding the putative location of the human homologue of monkey area AIP. According to one view, the human homologue of AIP may be located in the anterior part of the horizontal segment of the intraparietal sulcus or in a cortical region at the intersection between the postcentral and intraparietal sulci. For example, Binkofski et al. (1999) reported the location of the human homologue of AIP at x = -40, y = -40, z = 40, and Shikata et al. (2001) reported the location of the human AIP at x = -37, y = -40, z = 47 (for review of the coordinates of the human AIP in the anterior intraparietal sulcus see Frey et al., 2005, and Shikata et al., 2008). According to the findings of the present study, the postcentral and intraparietal sulci can appear to merge on the surface of the brain, but they are in fact always separated by a gyrus in the cortical depth (Figure 4i-j). In relation to our study, the stereotaxic coordinates of the human area AIP, as reported in the neuroimaging studies of Binkofski et al. (1999) and Shikata et al. (2001), place the human AIP at the gyrus between the postcentral and intraparietal sulci. However, there is another possibility that must also be entertained. The inferior segment of the postcentral sulcus, which has also been described as the vertical (ascending) part of the intraparietal sulcus (Cunningham, 1892), may relate to area AIP. We believe that this hypothesis must be entertained because area AIP in the monkey is located between the somatosensory area 2 and the most anterior part of the inferior parietal lobule. If the general anatomo-functional structure of the intraparietal sulcus is conserved between the monkey and the human, then the human homologue of the monkey area AIP may be expected at the transition between somatosensory area 2 and the most rostral part of the inferior parietal lobule, which is defined by the inferior part of the postcentral sulcus. There is one functional neuroimaging study by Simon et al. (2002) that reported tentative coordinates for the human AIP at x = - 60, y = -32, z = 36. These coordinates correspond to the inferior part of the postcentral sulcus in the current study.

In the human brain, the somatosensory cortical region extends from the superior longitudinal fissure to the lateral fissure and its boundaries are formed by the central sulcus, anteriorly, and the postcentral sulcus, posteriorly. As mentioned above, this somatosensory region is subdivided into cytoarchitectonic areas 3a, 3b, 1 and 2 (Brodmann, 1909; Geyer et al., 1999; Grefkes et al., 2001). Area 3b (area PB) is classified as the granulous koniocortex, while areas 1 and 2 belong to the homotypic isocortex. Although sometimes all of the postcentral gyrus somatosensory region is referred to as SI (primary somatosensory region), because the classical stimulation research in patients and monkeys did not have the resolution to distinguish effects

due to the stimulation of different architectonic areas (Penfield and Rasmussen, 1952; Woolsey et al., 1979), in fact only the granulous cortical area 3b should be referred to as the primary somatosensory cortex (Kaas, 1983). In addition to their difference in cytoarchitecture, areas 3a, 3b, 1 and 2 receive inputs from different submodalities (Merzenich et al., 1978; Kaas, 1983). Area 3a receives afferents from deep subcutaneous receptors, primarily muscle spindles. Area 3b receives inputs from rapidly and slowly adapting cutaneous receptors and area 1 afferents from rapidly adapting cutaneous receptors. Area 2 receives inputs from deep receptors in joints (Merzenich et al., 1978; Kaas, 1983). Physiological studies in monkeys have established that each architectonic area within the somatosensory cortex contains an orderly arranged representation of the various parts of the body (Whitsel et al., 1971; Merzenich et al., 1978; Kaas et al., 1979; Kaas, 1983).

The estimated dorsal to ventral arrangement of bodily representations in the human postcentral somatosensory cortex, based on the functional neuroimaging literature, is the following: toes, ankle, knee, midline trunk, hand, lips and teeth, tongue. We compared the stereotaxic coordinates of sensory representations of different parts of the body (see Table 10) with the averaged estimates of the stereotaxic coordinates of the four submerged plis de passage of the postcentral sulcus based on the present study (see Table 2) in order to examine a functional-anatomical relationship between the bodily representations and their posterior boundaries that are formed by the segments of the postcentral sulcus. Sensorimotor representations of the toes, ankle, knee and the entire foot are located on the postcentral gyrus above the first submerged pli de passage of the postcentral sulcus, anterior to the dorsal part of the first segment of the postcentral sulcus. Their representative locations approach the superior longitudinal fissure on the lateral and medial brain surface (see Tables 2 and 10). Activation peaks of sensory representations of the midline trunk are located close to the first submerged pli de passage of the postcentral sulcus and between the first and second segments of the postcentral sulcus. Sensory representations of the fingers and the hand are located between the first and second submerged plis de passage, anterior to the second segment of the postcentral sulcus. The lips, teeth and tongue are represented in the sensory cortex anterior to the third segment of the postcentral sulcus, between the second and third submerged plis de passage. The tip of the tongue is represented between the third and fourth submerged plis de passage, anterior to the fourth segment of the postcentral sulcus (see Tables 2 and 10).

In nearly half of all examined hemispheres (47.5%) both types of interrupting gyri, i.e. submerged plis de passage and visible gyri, occurred at the stereotaxic location of the third submerged pli de passage, which separates somatosensory representation of the hand dorsally from the representation of the face ventrally. Visible gyri occurred more often at the location of the first submerged pli de passage, which separates somatosensory representations of the toes, knee and ankle dorsally from the representation of the hand ventrally.

In one third of all hemispheres examined, there was a sulcus of variable length located anterior to the postcentral sulcus on the most ventral part of the postcentral gyrus (Figure 15). We refer to this sulcus as the transverse postcentral sulcus because it appears to correspond to the sulcus postcentralis (retrocentralis) transversus of Eberstaller (see Cunningham, 1892). Cunningham calls the sulcus postcentralis transversus the lowermost part of the postcentral sulcus, which may join superficially the inferior postcentral sulcus, but always remains separated from it by a deep annectant gyrus. In the brains examined in the current study, the transverse postcentral sulcus had a vertical dorso-ventral orientation and it was often placed in parallel with the postcentral sulcus. It was most frequently located in hemispheres where the postcentral sulcus terminated around the third submerged pli de passage. In these hemispheres, the transverse postcentral sulcus originated next to the second submerged pli de passage. In those brains where the postcentral sulcus terminated close to the fourth submerged pli de passage or ventral to it, the transverse postcentral sulcus was absent. Thus, we suggest that the transverse postcentral sulcus is an inferior segment of the postcentral sulcus which may or may not merge with the postcentral sulcus deep inside the fundus. Since the transverse postcentral sulcus is located next to the somatosensory face area, it may separate an anterior part of the postcentral gyrus from a posterior part of the postcentral gyrus that may play a different functional role related to the orofacial region of the body. Analysis of the stereotaxic coordinates of somatosensory representations of the lips, teeth and tongue (see Table 10) always placed them anterior to the transverse postcentral sulcus, which was determined from the anatomical observation of this sulcus in 40 human MRI brain volumes (unpublished observation). Therefore, it is suggested that the transverse postcentral sulcus is a morphological landmark separating the sensorimotor representation of the face from the posterior parietal cortex.

The present study investigated, in the MNI proportional stereotaxic space, the morphological structure of the postcentral sulcus and its relationship with the neighboring sulci. The results of this anatomical work may be used to relate specific functional activations acquired

in neuroimaging studies and registered to the standardized proportional stereotaxic space to details of sulcal and gyral anatomy of the anterior parietal lobe in the same stereotaxic space. A clear relationship between a specific type of functional activity and the local sulcal morphology can help clarify the functional organization of the cerebral cortex.

Acknowledgements

This research was supported by Canadian Institutes of Health Research (CIHR) grant MOP-14620 to M. Petrides.

References

Amiez, C., Kostopoulos, P., Champod, A. S., & Petrides, M. (2006). Local morphology predicts functional organization of the dorsal premotor region in the human brain. *The Journal of Neuroscience, 26*(10), 2724-2731.

Baumann, M. A., Fluet, M. C., & Scherberger, H. (2009). Context-specific grasp movement representation in the macaque anterior intraparietal area. *The Journal of Neuroscience*, *29*(20), 6436-6448.

Binkofski, F., Dohle, C., Posse, S., Stephan, K. M., Hefter, H., Seitz, R. J., & Freund, H. J. (1998). Human anterior intraparietal area subserves prehension A combined lesion and functional MRI activation study. *Neurology, 50*(5), 1253-1259.

Binkofski, F., Buccino, G., Posse, S., Seitz, R. J., Rizzolatti, G., & Freund, H. J. (1999). A fronto-parietal circuit for object manipulation in man: evidence from an fMRI-study. *European Journal of Neuroscience, 11*(9), 3276-3286.

Blatow, M., Nennig, E., Durst, A., Sartor, K., & Stippich, C. (2007). fMRI reflects functional connectivity of human somatosensory cortex. *Neuroimage, 37*(3), 927-936.

Boling, W., Olivier, A., Bittar, R. G., & Reutens, D. (1999). Localization of hand motor activation in Broca's pli de passage moyen. *Journal of Neurosurgery, 91*(6), 903-910.

Boling, W., Reutens, D. C., & Olivier, A. (2002). Functional topography of the low postcentral area. *Journal of Neurosurgery*, *97*(2), 388-395.

Brodmann, K. (1909). *Vergleichende Lokalisation der Grosshirnrinde in ihren Prinzipien dargestellt aufgrund des Zellenaufbaus*. Leipzig: Barth.

Chiavaras, M. M., & Petrides, M. (2000). Orbitofrontal sulci of the human and macaque monkey brain. *Journal of Comparative Neurology*, *422*(1), 35-54.

Collins, D. L., Neelin, P., Peters, T. M., & Evans, A. C. (1994). Automatic 3D intersubject registration of MR volumetric data in standardized Talairach space. *Journal of Computer Assisted Tomography, 18*(2), 192-205.

Connolly, C. J. (1950). *External morphology of the primate brain*. Springfield: Charles C Thomas.

Cunningham, D.J. 1892. *Contribution to the surface anatomy of the cerebral hemispheres by D. J. C., with a chapter upon cranio-cerebral topography by Victory Horsley*. Dublin: Royal Irish Academy.

Duvernoy, H. M., Cabanis, E. A., & Bourgouin, P. (1991). *The human brain: surface, three-dimensional sectional anatomy and MRI*. Wien: Springer-Verlag.

Eberstaller, O. (1890). *Das Stirnhirn*. Wien: Urban & Schwarzenberg.

Economo, C. (2009). *Cellular structure of the human cerebral cortex*. Basel: Karger Medical and Scientific Publishers.

Economo, C., & Koskinas, G. N. (1925). *Die Cytoarchitektur der Hirnrinde des erwachsenen Menschen*. Wien: Springer.

Eickhoff, S. B., Amunts, K., Mohlberg, H., & Zilles, K. (2006). The human parietal operculum. II. Stereotaxic maps and correlation with functional imaging results. *Cerebral Cortex, 16*(2), 268-279.

Smith, G. E. (1907). A new topographical survey of the human cerebral cortex, being an account of the distribution of the anatomically distinct cortical areas and their relationship to the cerebral sulci. *Journal of Anatomy and Physiology, 41*(Pt 4), 237-254.

Evans, A. C., Collins, D. L., & Milner, B. (1992). An MRI-based stereotactic brain atlas from 300 young normal subjects. Proceedings of the 22nd Annual Symposium of the Society for Neuroscience, Anaheim, CA, p 408.

Fabri, M., Polonara, G., Salvolini, U., & Manzoni, T. (2005). Bilateral cortical representation of the trunk midline in human first somatic sensory area. *Human Brain Mapping*, *25*(3), 287-296.

Ferretti, A., Del Gratta, C., Babiloni, C., Caulo, M., Arienzo, D., Tartaro, A., Rossini, P. M., & Luca Romani, G. (2004). Functional topography of the secondary somatosensory cortex for nonpainful and painful stimulation of median and tibial nerve: an fMRI study. *Neuroimage*, *23*(3), 1217-1225.

Frey, S. H., Vinton, D., Norlund, R., & Grafton, S. T. (2005). Cortical topography of human anterior intraparietal cortex active during visually guided grasping. *Cognitive Brain Research*, *23*(2), 397-405.

Gallese, V., Murata, A., Kaseda, M., Niki, N., & Sakata, H. (1994). Deficit of hand preshaping after muscimol injection in monkey parietal cortex. *Neuroreport*, *5*(12), 1525-1529.

Germann, J., Robbins, S., Halsband, U., & Petrides, M. (2005). Precentral sulcal complex of the human brain: morphology and statistical probability maps. *Journal of Comparative Neurology*, *493*(3), 334-356.

Geyer, S., Schleicher, A., & Zilles, K. (1999). Areas 3a, 3b, and 1 of human primary somatosensory cortex: 1. Microstructural organization and interindividual variability. *Neuroimage*, *10*(1), 63-83.

Geyer, S., Schormann, T., Mohlberg, H., & Zilles, K. (2000). Areas 3a, 3b, and 1 of human primary somatosensory cortex: 2. Spatial normalization to standard anatomical space. *Neuroimage*, *11*(6), 684-696.

Grefkes, C., Geyer, S., Schormann, T., Roland, P., & Zilles, K. (2001). Human somatosensory area 2: observer-independent cytoarchitectonic mapping, interindividual variability, and population map. *Neuroimage, 14*(3), 617-631.

Grefkes, C., Weiss, P. H., Zilles, K., & Fink, G. R. (2002). Crossmodal processing of object features in human anterior intraparietal cortex: an fMRI study implies equivalencies between humans and monkeys. *Neuron, 35*(1), 173-184.

Grefkes, C., Ritzl, A., Zilles, K., & Fink, G. R. (2004). Human medial intraparietal cortex subserves visuomotor coordinate transformation. *Neuroimage, 23*(4), 1494-1506.

Huttner, H. B., Lohmann, G., & Yves von Cramon, D. (2005). Magnetic resonance imaging of the human frontal cortex reveals differential anterior–posterior variability of sulcal basins. *Neuroimage, 25*(2), 646-651.

Kaas, J. H. (1983). What, if anything, is SI? Organization of first somatosensory area of cortex. *Physiological Reviews, 63*(1), 206-231.

Kaas, J. H., Nelson, R. J., Sur, M., Lin, C. S., & Merzenich, M. M. (1979). Multiple representations of the body within the primary somatosensory cortex of primates. *Science, 204*(4392), 521-523.

Kalaska, J. F. (1996). Parietal cortex area 5 and visuomotor behavior. *Canadian Journal of Physiology and Pharmacology, 74*(4), 483-498.

Kapreli, E., Athanasopoulos, S., Papathanasiou, M., Van Hecke, P., Kelekis, D., Peeters, R., Strimpakos, N., & Sunaert, S. (2007). Lower limb sensorimotor network: issues of somatotopy and overlap. *Cortex, 43*(2), 219-232.

Lohmann, G., & von Cramon, D. Y. (2000). Automatic labelling of the human cortical surface using sulcal basins. *Medical Image Analysis, 4*(3), 179-188.

Lotze, M., Seggewies, G., Erb, M., Grodd, W., & Birbaumer, N. (2000). The representation of articulation in the primary sensorimotor cortex. *Neuroreport*, *11*(13), 2985-2989.

MacDonald, D., Avis, D., & Evans, A. C. (1994, September). Multiple surface identification and matching in magnetic resonance images. In *Visualization in Biomedical Computing 1994* (pp. 160-169). International Society for Optics and Photonics.

MacDonald, D. (1996). Program for display and segmentation of surfaces and volumes. McConnell Brain Imaging Center, Montreal Neurological Institute, Montreal, Quebec, Canada [software available from http://www.bic.mni.mcgill.ca].

Mazziotta, J. C., Toga, A. W., Evans, A., Fox, P., & Lancaster, J. (1995a). A probabilistic atlas of the human brain: theory and rationale for its development the international consortium for brain mapping (ICBM). *Neuroimage*, *2*(2PA), 89-101.

Mazziotta, J. C., Toga, A. W., Evans, A. C., Fox, P. T., & Lancaster, J. L. (1995b). Digital brain atlases. *Trends in Neurosciences*, *18*(5), 210-211.

Merzenich, M. M., Kaas, M., Sur, M., & Lin C. S. (1978). Double representation of the body surface within cytoarchitectonic areas 3b and 2 in Sl in the owl monkey (Aotus trivirgatus). *Journal of Comparative Neurology*, *181*, 41-74.

Miyamoto, J. J., Honda, M., Saito, D. N., Okada, T., Ono, T., Ohyama, K., & Sadato, N. (2006). The representation of the human oral area in the somatosensory cortex: a functional MRI study. *Cerebral Cortex*, *16*(5), 669-675.

Nakamura, A., Yamada, T., Goto, A., Kato, T., Ito, K., Abe, Y., Kachi, T., & Kakigi, R. (1998). Somatosensory homunculus as drawn by MEG. *Neuroimage*, *7*(4), 377-386.

Ono, M., Kubik, S., & Abernathey, C. D. (1990). *Atlas of the cerebral sulci*. Stuttgart: Thieme.

Petrides, M., & Pandya, D. N. (2002). Association pathways of the prefrontal cortex and functional observations. In D. T. Stuss & R. T. Knight (Eds.), *Principles of Frontal Lobe Function* (pp. 31-50). New York: Oxford University Press.

Penfield, W., & Rasmussen, T. (1950). *The cerebral cortex of man; a clinical study of localization of function*. New York: The Macmillan Company.

Regis, J., Mangin, J. F., Ochiai, T., Frouin, V., Riviere, D., Cachia, A., Tamura, M., & Samson, Y. (2005). "Sulcal root" generic model: a hypothesis to overcome the variability of the human cortex folding patterns. *Neurologia Medico-Chirurgica*, *45*(1), 1-17.

Retzius, G. (1896). *Das Menschenhirn; Studien in der makroskopischen Morphologie*. Stockholm: Norstedt and Soener.

Sakata, H., Taira, M., Murata, A., & Mine, S. (1995). Neural mechanisms of visual guidance of hand action in the parietal cortex of the monkey. *Cerebral Cortex*, *5*(5), 429-438.

Sarkissov, S. A., Filimonoff, I. N., Kononowa, E. P., Preobraschenskaja, I. S., & Kukuew, L. A. (1955). *Atlas of the cytoarchitectonics of the human cerebral cortex*. Moscow: Medgiz.

Scheperjans, F., Grefkes, C., Palomero-Gallagher, N., Schleicher, A., & Zilles, K. (2005). Subdivisions of human parietal area 5 revealed by quantitative receptor autoradiography: a parietal region between motor, somatosensory, and cingulate cortical areas. *Neuroimage*, *25*(3), 975-992.

Shikata, E., Hamzei, F., Glauche, V., Knab, R., Dettmers, C., Weiller, C., & Büchel, C. (2001). Surface orientation discrimination activates caudal and anterior intraparietal sulcus in humans: an event-related fMRI study. *Journal of Neurophysiology*, *85*(3), 1309-1314.

Shikata, E., McNamara, A., Sprenger, A., Hamzei, F., Glauche, V., Büchel, C., & Binkofski, F. (2008). Localization of human intraparietal areas AIP, CIP, and LIP using surface orientation and saccadic eye movement tasks. *Human Brain Mapping*, *29*(4), 411-421.

Simon, O., Mangin, J. F., Cohen, L., Le Bihan, D., & Dehaene, S. (2002). Topographical layout of hand, eye, calculation, and language-related areas in the human parietal lobe. *Neuron, 33*(3), 475-487.

Talairach, J., & Tournoux, P. (1988). *Co-planar stereotaxic atlas of the human brain*. Stuttgart, Germany: Thieme.

Toro, R., & Burnod, Y. (2005). A morphogenetic model for the development of cortical convolutions. *Cerebral Cortex, 15*(12), 1900-1913.

Van Essen, D. C. (1997). A tension-based theory of morphogenesis and compact wiring in the central nervous system. *Nature, 385,* 313-318.

Vogt, O. (1911). Die Myeloarchitectonik des Isocortex parietalis. *Journal für Psychologie und Neurologie, 19,* 107-118.

Welker, W. (1990). Why does cerebral cortex fissure and fold? A review of determinants of gyri and sulci. In E. G. Jones & A. Peters (Eds.), *Cerebral cortex* (pp. 3-136). New York: Plenum Press.

Wenderoth, N., Debaere, F., Sunaert, S., Van Hecke, P., & Swinnen, S. P. (2004). Parieto-premotor areas mediate directional interference during bimanual movements. *Cerebral Cortex, 14*(10), 1153-1163.

Whitsel, B. L., Dreyer, D. A., & Roppolo, J. R. (1971). Determinants of body representation in postcentral gyrus of macaques. *Journal of Neurophysiology, 34,* 1018-1034.

Woolsey, C. N., Erickson, T. C., & Gilson, W. E. (1979). Localization in somatic sensory and motor areas of human cerebral cortex as determined by direct recording of evoked potentials and electrical stimulation. *Journal of Neurosurgery, 51*(4), 476-506.

Zhang, M., Mariola, E., Stilla, R., Stoesz, M., Mao, H., Hu, X., & Sathian, K. (2005). Tactile discrimination of grating orientation: fMRI activation patterns. *Human Brain Mapping, 25*(4), 370-377.

Abbreviations

Sulci and gyri

aIPS, anterior part of the horizontal segment of the intraparietal sulcus

CS, central sulcus

CingS, ascending (marginal) branch of the cingulate sulcus

dS, sulcus located dorsal to the PoCS

G-1st, gyrus which divides PoCS into 2 segments, superior and inferior PoCS. This gyrus is visible on the surface and in the fundus. It is located at the first submerged pli de passage.

iPoCS, inferior postcentral sulcus

iPrS, inferior precentral sulcus

IPS, intraparietal sulcus (horizontal segment and its branches)

LF, lateral fissure

LuS, lunate sulcus

mPoCS, middle postcentral sulcus

OpS, sulcus located on the parietal operculum (upper lip of the lateral fissure)

sFS, superior frontal sulcus

sPoCS, superior postcentral sulcus

POF, parieto-occipital fissure

posc, posterior subcentral sulcus

sPrS, superior precentral sulcus

SLF, superior longitudinal fissure

STS, superior temporal sulcus

TrS, transverse postcentral sulcus

Submerged plis de passage

3, third submerged pli de passage

4, fourth submerged pli de passage

1s, submerged gyrus at location of the first submerged pli de passage

1v, visible gyrus at location of the first submerged pli de passage

2s, submerged gyrus at location of the second submerged pli de passage

2v, visible gyrus at location of the second submerged pli de passage

3s, submerged gyrus at location of the third submerged pli de passage

3v, visible gyrus at location of the third submerged pli de passage

4s, submerged gyrus at location of the fourth submerged pli de passage

spdp, submerged pli de passage

Tables

Table 1. Incidence and distribution of segments of the postcentral sulcus (PoCS) among the left (LH) and right (RH) hemispheres of 40 MRI brain volumes

Type of PoCS Segmentation	**LH+RH**		**LH**		**RH**	
	Total # LH+RH	% 80 LH+RH	Total # LH	% 40 LH	Total # RH	% 40 RH
Continuous	11	13.75	3	7.5	8	20
Two segments	37	46.25	16	40	21	52.5
Three segments	22	27.50	12	30	10	25
Four segments	9	11.25	8	20	1	2.5
Five segments	1	1.25	1	2.5	0	0

Table 2. Averaged stereotaxic coordinates of four submerged plis de passage (submerged pdp) in the MNI proportional stereotaxic space

Structure	**Average MNI coordinates**					
	Left hemisphere			**Right hemisphere**		
	x	**y**	**z**	**x**	**y**	**z**
First submerged pdp*	-28	-34	54			
Second submerged pdp	-38	-31	43	36	-32	43
Third submerged pdp	-41	-27	35	45	-25	34
Fourth submerged pdp	-55	-18	28	52	-16	29

Note: * There were not enough data to determine the stereotaxic coordinates of the first submerged pli de passage in the right hemisphere.

Table 3. Incidence of the presence of submerged and visible gyri in the distinct locations of four submerged plis de passage (spdp) in the left (LH) and right (RH) hemispheres of 40 MRI brain volumes

Location	**LH**			**RH**			**LH+RH**	
	Total # LH	% 40 LH	% Total LH+RH	Total # RH	% 40 RH	% Total LH+RH	Total # LH+RH	% Total LH+RH
Submerged gyri								
1st spdp	6	15	85.71	1	2.5	14.29	7	8.75
2nd spdp	6	15	54.55	5	12.5	45.45	11	13.75
3rd spdp	18	45	60	12	30	40	30	37.5
4th spdp	10	25	62.5	6	15	37.5	16	20
Visible gyri								
1st spdp	16	40	69.57	7	17.5	30.43	23	28.75
2nd spdp	2	5	28.57	5	12.5	71.43	7	8.75
3rd spdp	5	12.5	62.5	3	7.5	37.5	8	10
4th spdp	2	5	50	2	5	50	4	5
Interrupting gyri (combined submerged and visible gyri)								
1st spdp	22	55	73.33	8	20	26.67	30	37.5
2nd spdp	8	20	44.44	10	25	55.56	18	22.5
3rd spdp	23	57.5	60.53	15	37.5	39.47	38	47.5
4th spdp	12	30	60	8	20	40	20	25

Table 4. Types of dorsal termination of the postcentral sulcus (PoCS) and their incidence in the left (LH) and right (RH) hemispheres of the human brain

Type of dorsal end of PoCS	**LH+RH**		**LH**		**RH**	
	Total # LH+RH	% 80 LH+RH	Total # LH	% 40 LH	Total # RH	% 40 RH
Dorsal end is regular	19	23.75	7	17.5	12	30
Dorsal end is bifurcated	55	68.75	31	77.5	24	60
Dorsal end has three branches	6	7.5	2	5	4	10
PoCS reaches the superior longitudinal fissure	23	28.75	11	27.5	12	30

Table 5. Patterns formed by the postcentral sulcus (PoCS) and the lateral fissure (LF) and their incidence in the left (LH) and right (RH) hemispheres of the human brain

PoCS relative to LF	**LH+RH**		**LH**		**RH**	
	Total # LH+RH	% 80 LH+RH	Total # LH	% 40 LH	Total # RH	% 40 RH
PoCS superficially merges with LF (i.e. gyrus separating the sulci is submerged)	24	30	13	32.5	11	27.5
PoCS does not superficially merge with LF (i.e. gyrus separating the sulci is visible)	56	70	27	67.5	29	72.5

Table 6. Patterns formed by the postcentral sulcus (PoCS) and the anterior part of the horizontal segment of the intraparietal sulcus (IPS) on the surface of the brain

PoCS and anterior IPS (surface-based analysis)	**LH+RH**		**LH**		**RH**	
	Total # LH+RH	% 80 LH+RH	Total # LH	% 40 LH	Total # RH	% 40 RH
IPS merges with continuous PoCS	25	31.25	10	25	15	37.5
IPS merges with superior PoCS	5	6.25	0	0	5	12.5
IPS merges with inferior PoCS	16	20	11	27.5	5	12.5
IPS merges with middle PoCS	2	2.5	2	5	0	0
IPS merges with superior and inferior PoCS	0	0	0	0	0	0
IPS is separated from all segments of PoCS by a visible gyrus	32	40	17	42.5	15	37.5

Table 7. Patterns formed by the postcentral sulcus (PoCS) and the ascending branch of the cingulate sulcus (CingS) in the left (LH) and right (RH) hemispheres of the human brain

PoCS and CingS	**LH+RH**		**LH**		**RH**	
	Total # LH+RH	% 80 LH+RH	Total # LH	% 40 LH	Total # RH	% 40 RH
CingS is seen on the lateral surface	33	41.25	19	47.5	14	35
CingS terminates anterior to PoCS or inside a bifurcation of PoCS	57	71.25	31	77.5	26	65
CingS terminates posterior to PoCS	23	28.75	9	22.5	14	35

Table 8. Types of sulci which are located dorsal to the postcentral sulcus (PoCS) and their patterns with the superior longitudinal fissure (SLF) in the left (LH) and right (RH) hemispheres of the human brain

Types of sulci located dorsal to PoCS	**LH+RH**		**LH**		**RH**	
	Total # LH+RH	% 80 LH+RH	Total # LH	% 40 LH	Total # RH	% 40 RH
Sulci dorsal to PoCS which reach SLF	27	33.75	17	42.5	10	25
Sulci dorsal to PoCS which *do not* reach SLF	9	11.25	3	7.5	6	15

Table 9. Types of sulci located on the inferior postcentral gyrus (infPoCG) and their incidence in the left (LH) and right (RH) hemispheres of the human brain

Types of sulci on infPoCG	**LH+RH**		**LH**			**RH**		
	Total # LH+RH	% 80 LH+RH	Total # LH	% 40 LH	% 80 LH+RH	Total # RH	% 40 RH	% 80 LH+RH
Transverse post-central sulcus	26	32.5	10	25	38.5	16	40	61.5
No sulci on infPoCG	36	45	16	40	44.4	20	50	55.6
All other sulci (posterior subcentral sulcus, opercular sulci)	43	53.5	26	65	60.5	17	42.5	39.5

Table 10. Representation of different body regions in the contralateral primary somatosensory cortex

Study	**Brain region**	**Left hemisphere stereotaxic coordinates**			**Right hemisphere stereotaxic coordinates**		
		x	**y**	**z**	**x**	**y**	**z**
Kapreli et al. 2007*	Toes	– 6.1	– 42.9	72.3	6.1	– 39.2	71.8
	Ankle	– 6.8	– 41.3	70.9	6.4	– 38.3	70.1
	Knee	– 9.9	– 39.6	68.4	10.1	– 36.7	68.8
Ferretti et al. 2004	Foot	– 4	– 42	59			
Fabri et al. 2005	Lateral midline trunk				30	– 33	55
	Posterior midline trunk				32	– 33	53
	Anterior midline trunk				34	– 25	53
Fabri et al. 2005	Hand				41	– 25	54
Ferretti et al. 2004	Hand	– 34	– 35	50			
Blatow et al. 2007	Fingers	– 49	– 21	46	49	– 19	46
Kapreli et al. 2007*	Finger	– 38.7	– 26.5	53.6	38.5	– 23.7	50.4
Blatow et al. 2007	Lips	– 56	– 17	36	52	– 14	38
Lotze et al. 2000	Lip pursing	– 52	– 16	38	54	– 6	38
Miyamoto et al. 2006	Rostral lip	– 55.5	– 11.3	41.7			
	Middle lip	– 58.3	– 16.0	39.4			
	Caudal lip	– 58.0	– 21.2	39.1			
	Rostral tooth	– 55.8	– 11.0	40.4			
	Middle tooth	– 57.6	– 16.1	39.4			
	Caudal tooth	– 56.7	– 22.2	40.8			
	Rostral tongue	– 57.1	– 9.8	38.5			
	Middle tongue	– 58.1	– 15.4	38.2			
	Caudal tongue	– 57.9	– 21.1	39.1			
Lotze et al. 2000	Tip of tongue	– 52	2	32	66	– 2	24

Note: * In Kapreli et al. (2007) representations are shown for the primary sensorimotor cortex.

Figures

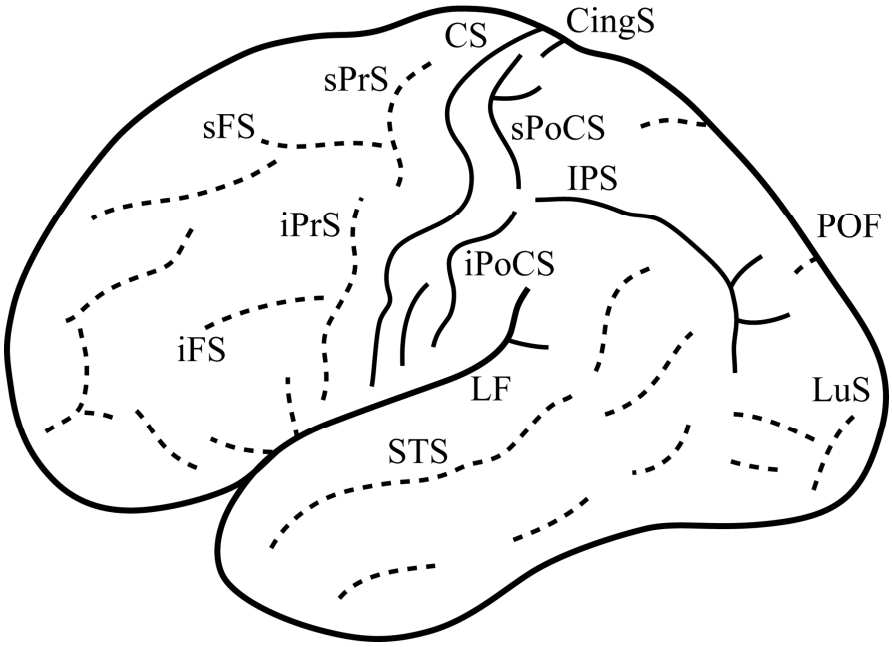

Figure 1. Schematic representation of the main sulci on the lateral surface of the human brain.

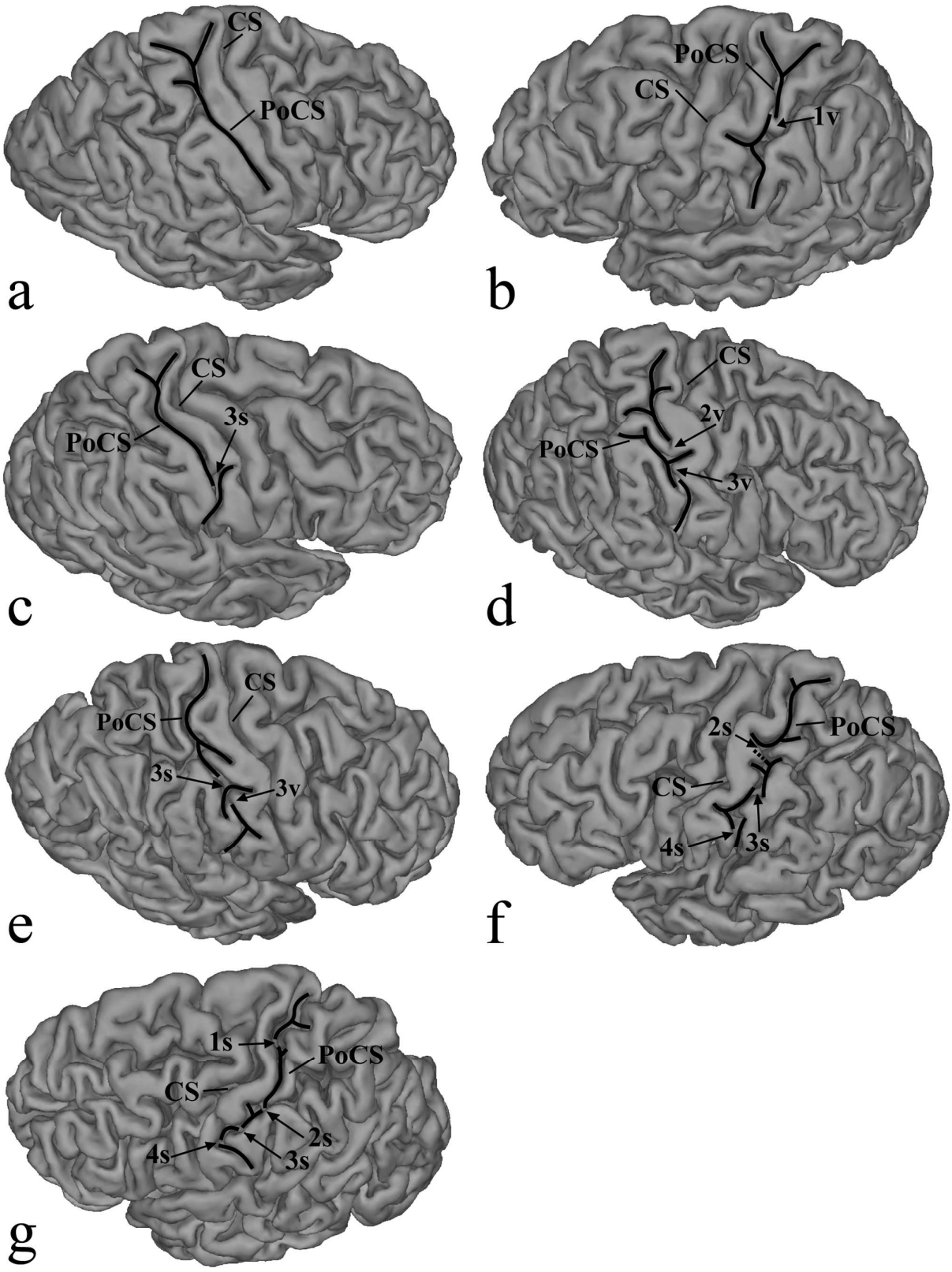
CS
PoCS
a
PoCS
CS
1v
b
CS
3s
PoCS
c
CS
2v
PoCS
3v
d
CS
PoCS
3s
3v
e
2s
PoCS
CS
4s
3s
f
1s
PoCS
CS
2s
4s
3s
g

Figure 2. Segmentation of the postcentral sulcus on the surface of the brain and in the fundus. This figure illustrates 7 different types of interaction between the surface-based and cross-section analyses with regard to segmentation patterns of the postcentral sulcus. All panels show 3D reconstructions of MRI brain volumes used in this study. In (**a**), (**b**) and (**d**) the postcentral sulcus is found to contain one, two and three segments, respectively, using both methodologies. In (**c**), (**e**), (**f**) and (**g**) the cross section analysis determined that the postcentral sulcus is divided into a larger number of segments in the fundus than on the surface of the brain. In (**a**) the postcentral sulcus is continuous both in the fundus and on the surface. In (**b**) the postcentral sulcus is divided into two segments by a visible gyrus located at the 1st submerged pli de passage [1v]. In (**c**) the postcentral sulcus is continuous on the surface of the brain, but it is divided into two segments by a submerged gyrus located at the 3rd submerged pli de passage [3s]. In (**d**) the postcentral sulcus consists of 3 segments separated by two visible gyri at the 2nd and 3rd submerged plis de passage [2v; 3v]. In (**e**) the postcentral sulcus appears to consist of two segments on the surface of the brain, but it is divided into three segments in the fundus. The first interrupting gyrus at the 3rd submerged pli de passage is submerged [3s] and the second interrupting gyrus at the 3rd submerged pli de passage is visible on the brain surface [3v]. In (**f**) the postcentral sulcus appears continuous on the surface of the brain, but it is divided into four segments by submerged gyri in its fundus. The submerged gyri are located at the 2nd, 3rd and 4th submerged plis de passage [2s; 3s; 4s]. In (**g**) the postcentral sulcus appears continuous on the surface of the brain, but it is divided into five segments by submerged gyri in its fundus. The submerged gyri are located at the 1st, 2nd, 3rd and 4th submerged plis de passage [1s; 2s; 3s; 4s].

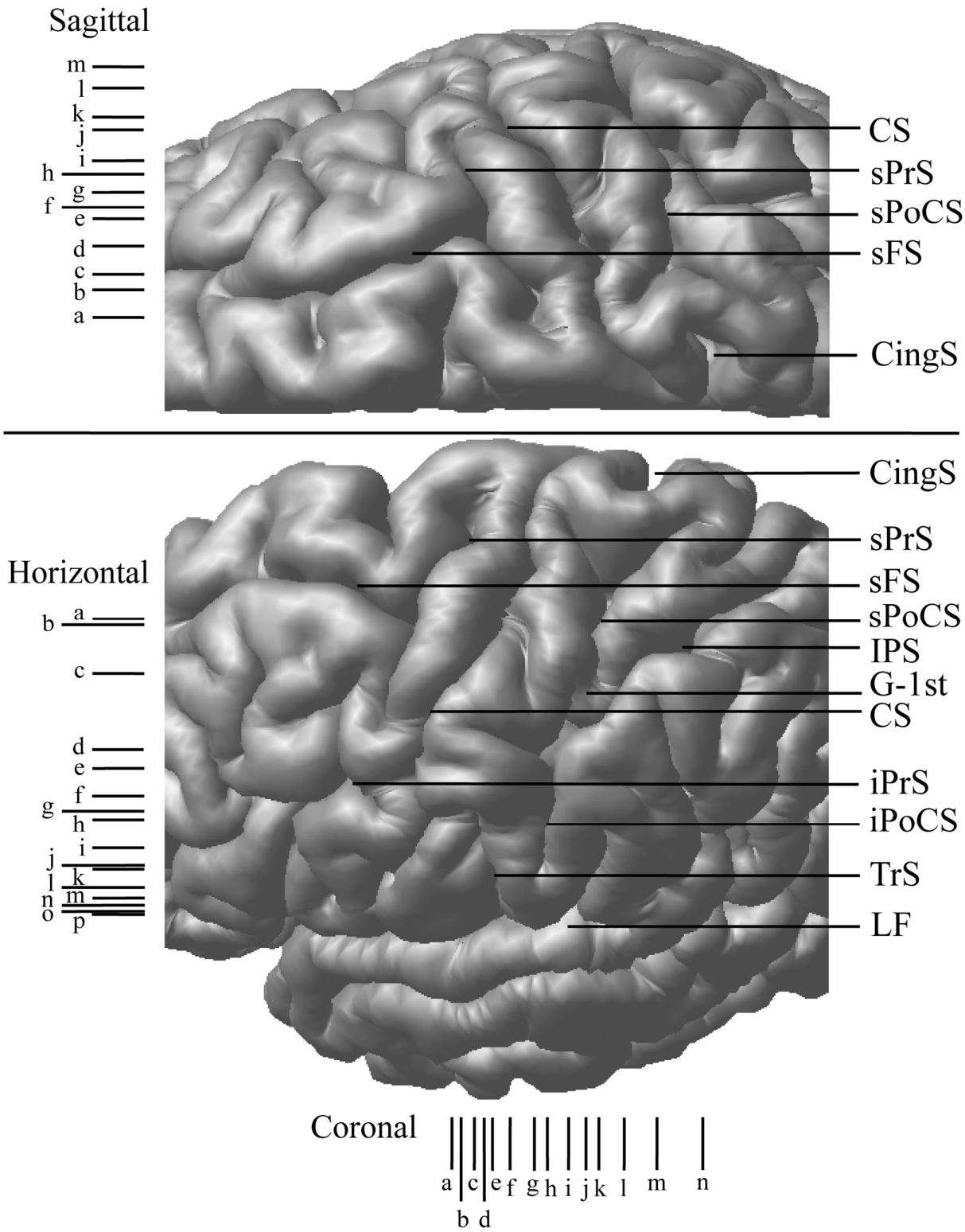
Sagittal
m
l
k
j
i
h
g
f
e
d
c
b
a
CS
sPrS
sPoCS
sFS
CingS
Horizontal
b
a
c
d
e
f
g
h
i
j
k
l
m
n
o
p
CingS
sPrS
sFS
sPoCS
IPS
G-1st
CS
iPrS
iPoCS
TrS
LF
Coronal
a
b
c
d
e
f
g
h
i
j
k
l
m
n

Figure 3. Three-dimensional reconstruction of the left hemisphere of the MRI brain volume (case 1) used in the current study. Horizontal sections are shown in Figure 4, coronal sections in Figure 5 and sagittal sections in Figure 6.

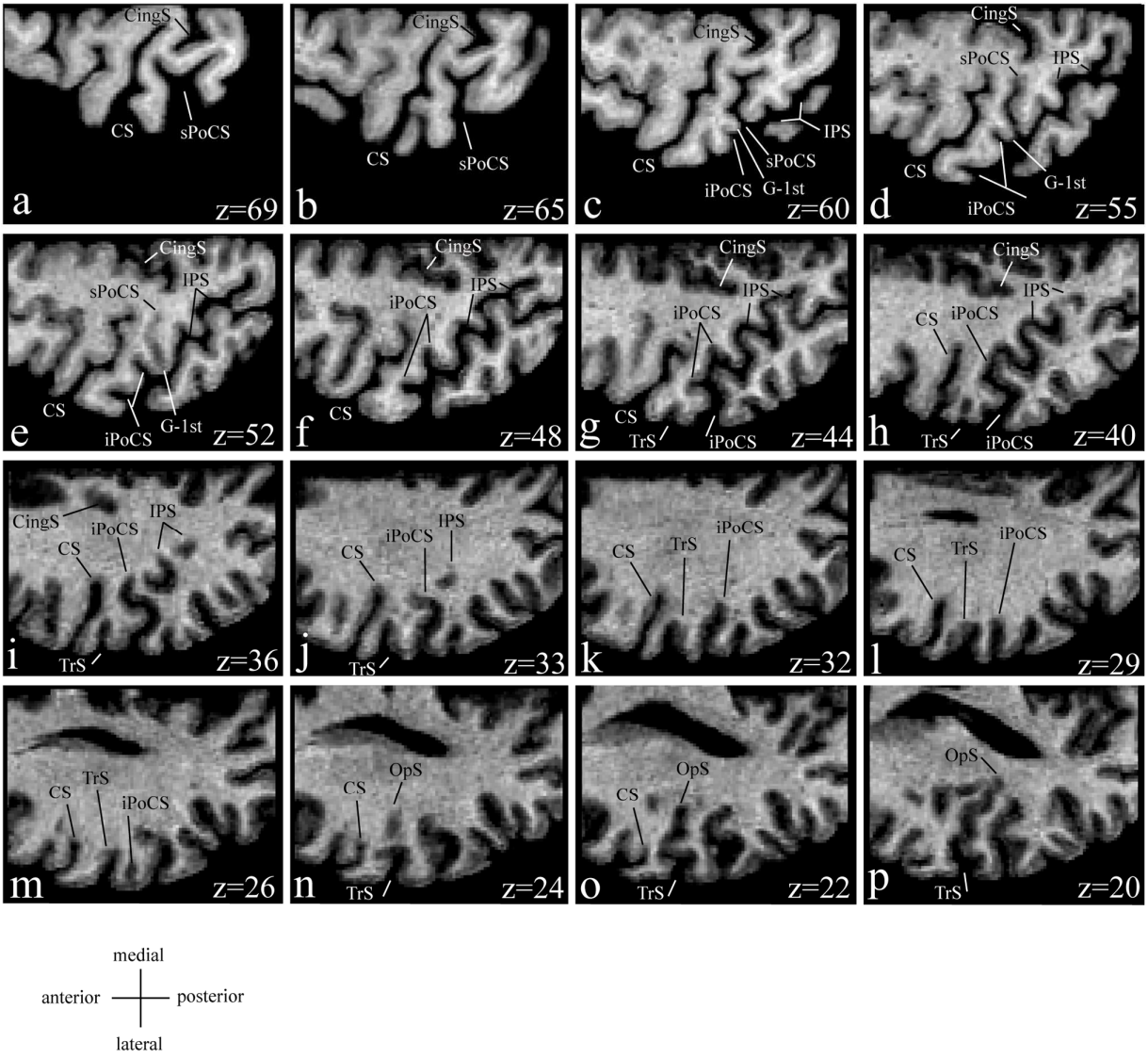

Figure 4. Horizontal sections from the left hemisphere of the MRI brain volume (case 1) with the sulci of interest identified. The level in the dorso-ventral dimension (z coordinate) is given in millimetres for each section.

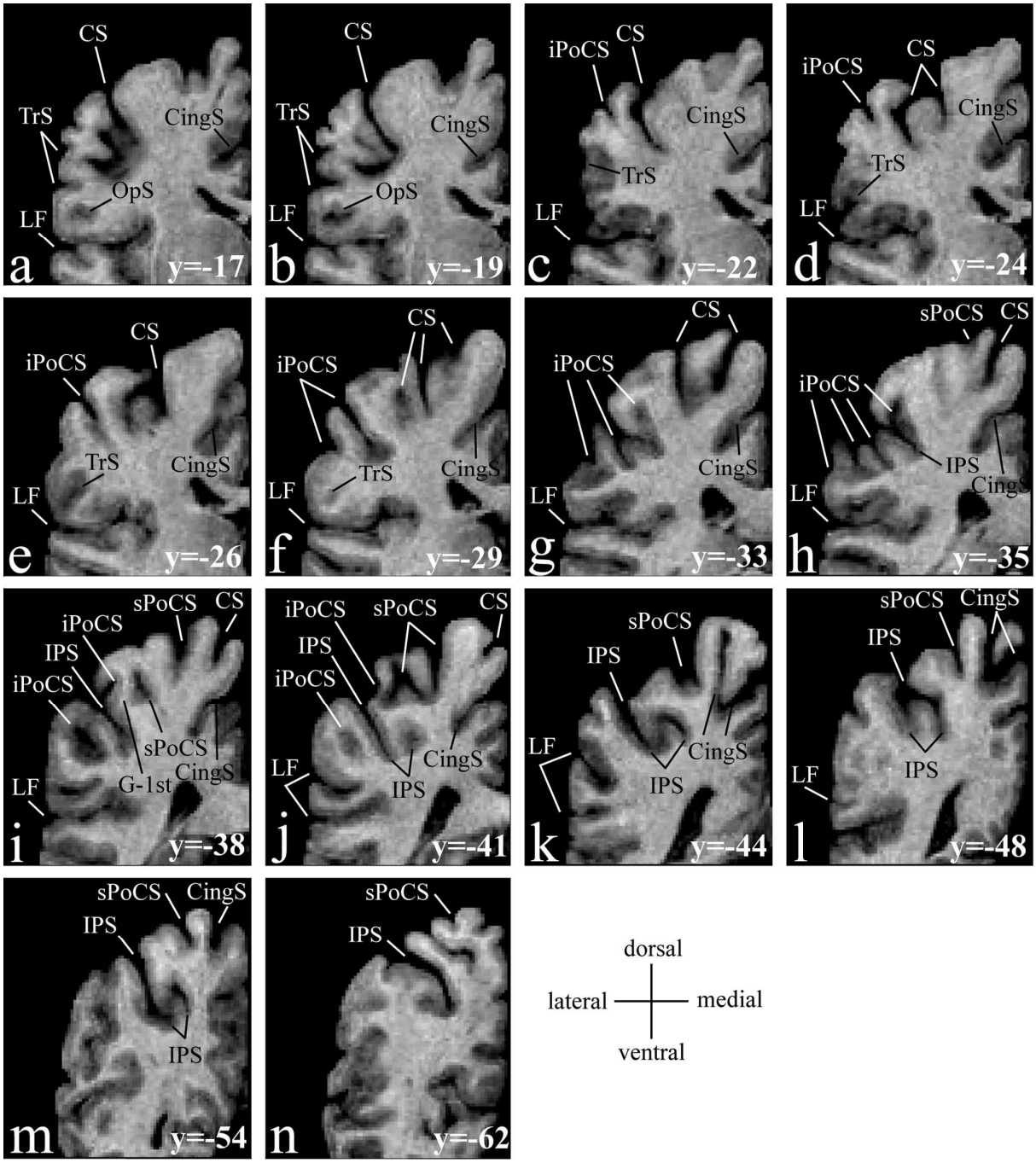

Figure 5. Coronal sections from the left hemisphere of the MRI brain volume (case 1) with the sulci of interest identified. The level in the rostro-caudal dimension (y coordinate) is given in millimetres for each section.

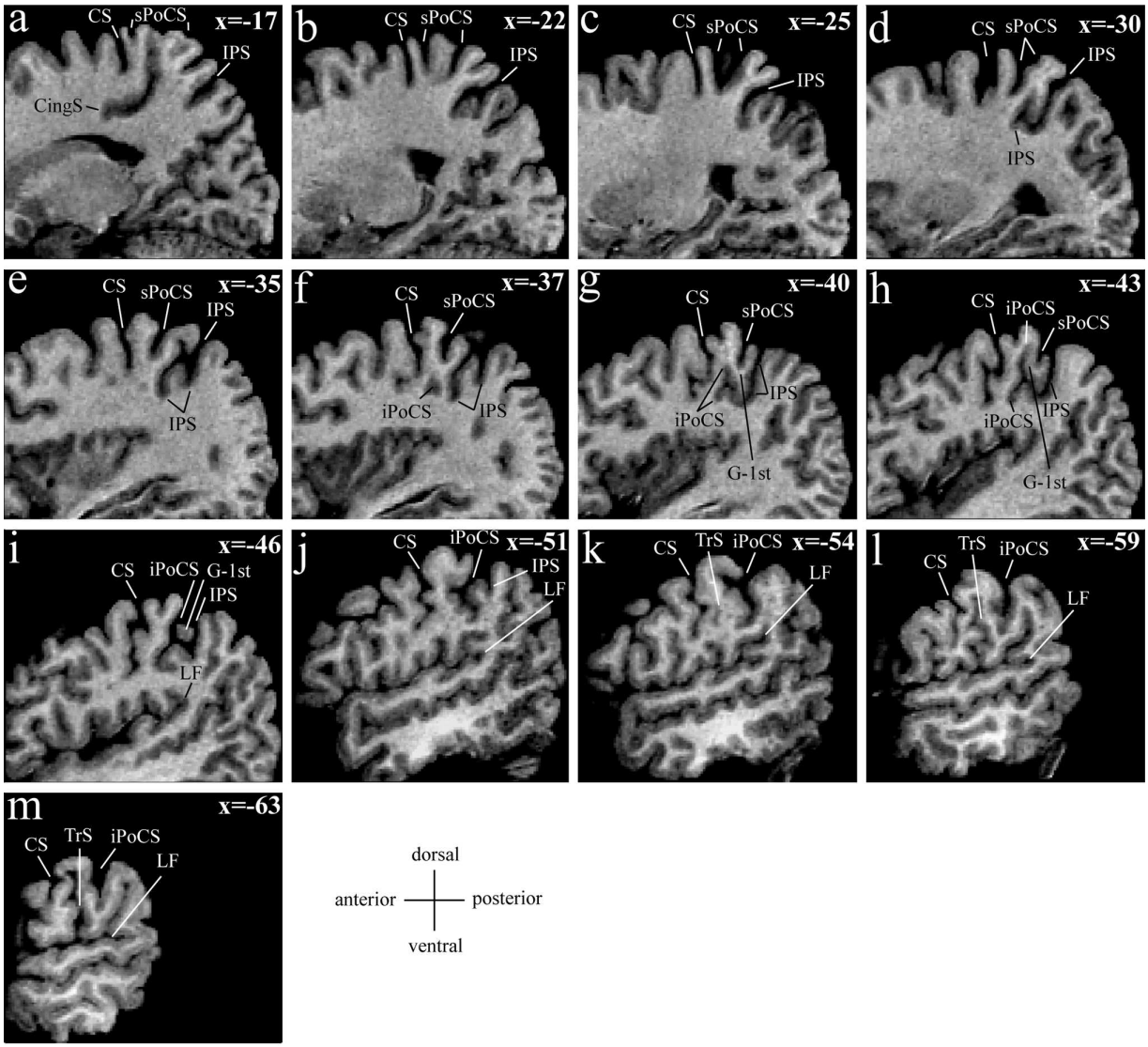

Figure 6. Sagittal sections from the left hemisphere of the MRI brain volume (case 1) with the sulci of interest identified. The level in the medio-lateral dimension (x coordinate) is given in millimetres for each section.

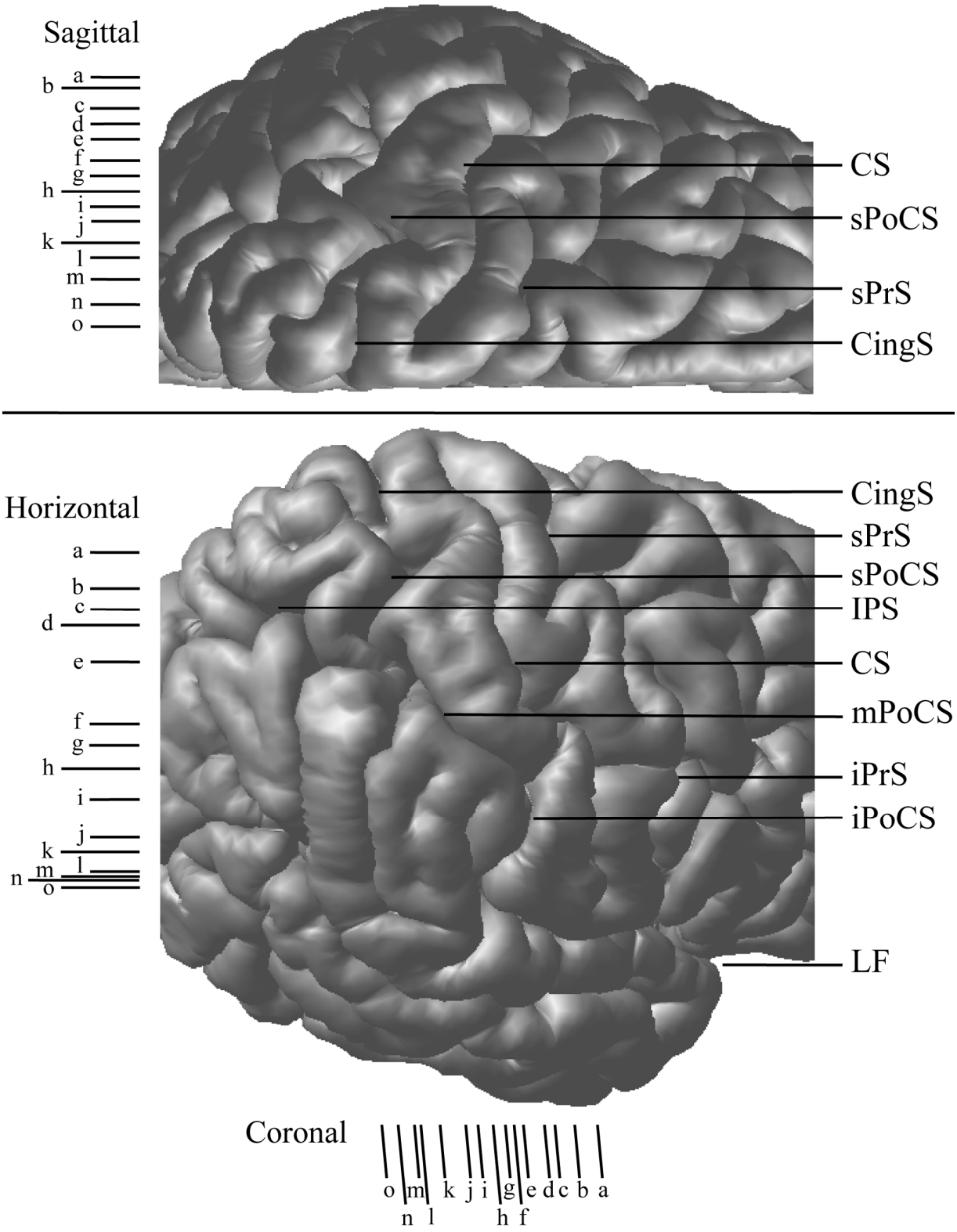
Sagittal
a
b
c
d
e
f
g
h
i
j
k
l
m
n
o
CS
sPoCS
sPrS
CingS
Horizontal
a
b
c
d
e
f
g
h
i
j
k
l
m
n
o
CingS
sPrS
sPoCS
IPS
CS
mPoCS
iPrS
iPoCS
LF
Coronal
o m k j i g e d c b a
n l h f

Figure 7. Three-dimensional reconstruction of the right hemisphere of the MRI brain volume (case 2). Horizontal sections are shown in Figure 8, coronal sections in Figure 9 and sagittal sections in Figure 10.

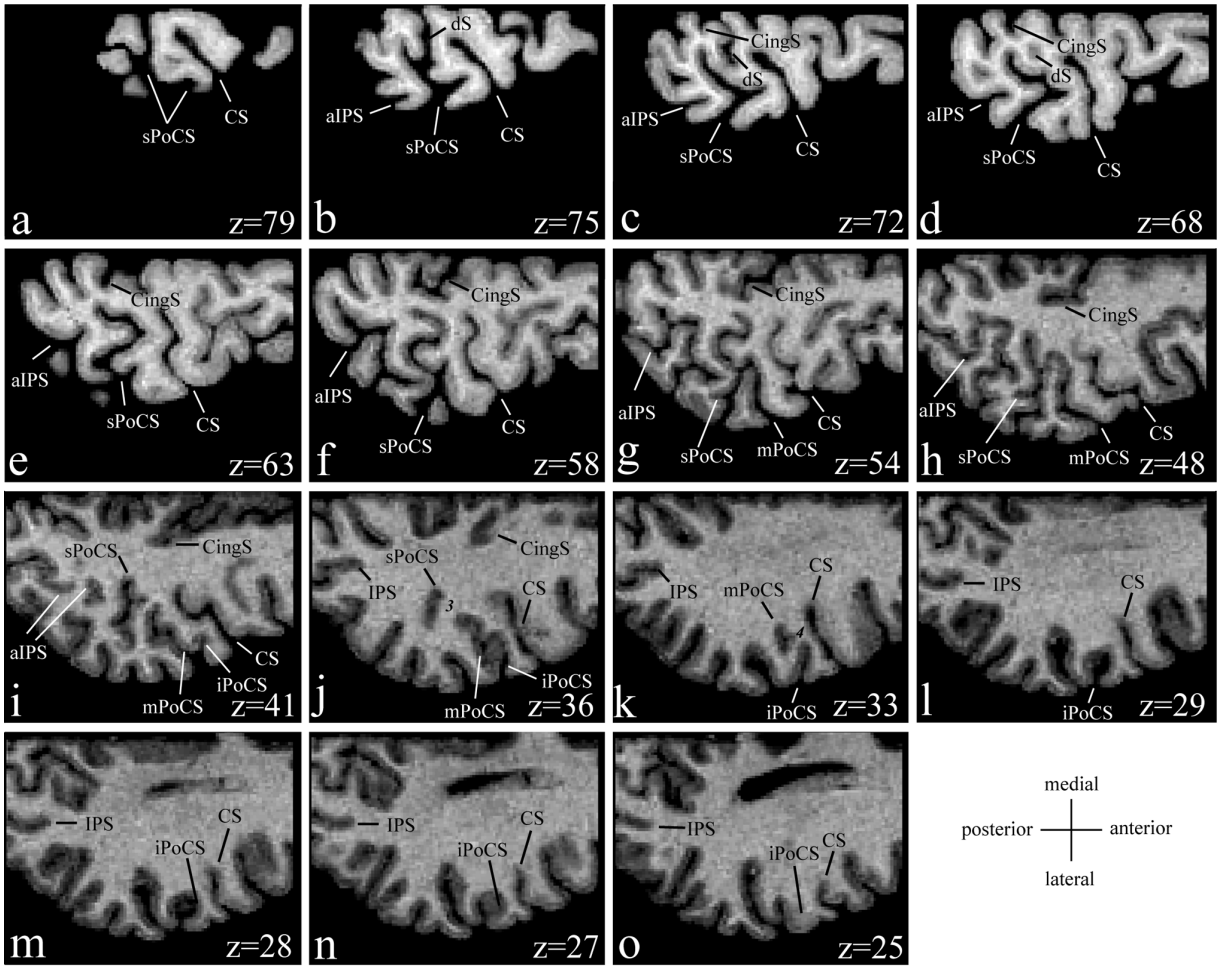

Figure 8. Horizontal sections from the right hemisphere of the MRI brain volume (case 2) with the sulci of interest identified. The level in the dorso-ventral dimension (z coordinate) is given in millimetres for each section.

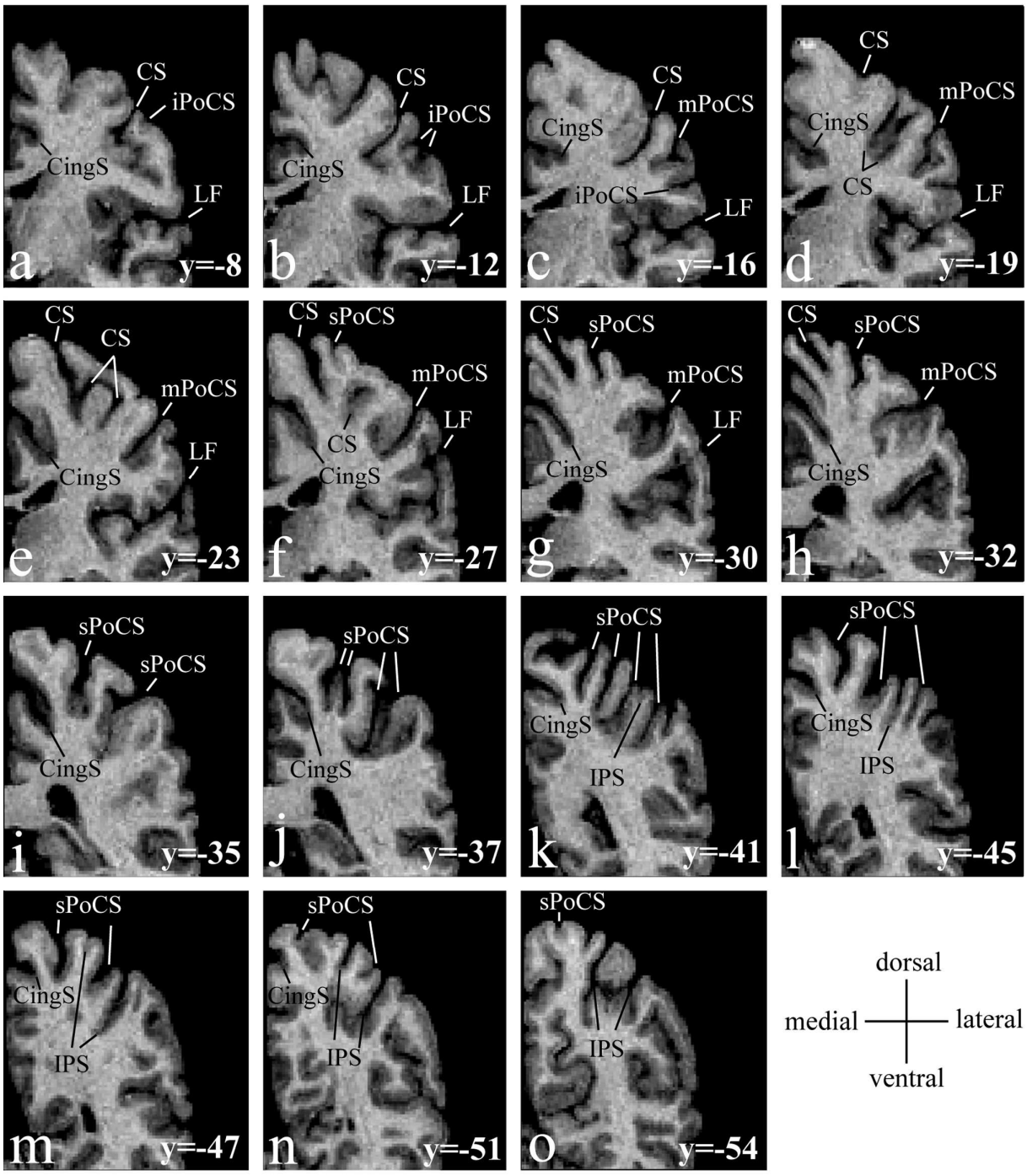

Figure 9. Coronal sections from the right hemisphere of the MRI brain volume (case 2) with the sulci of interest identified. The level in the rostro-caudal dimension (y coordinate) is given in millimetres for each section.

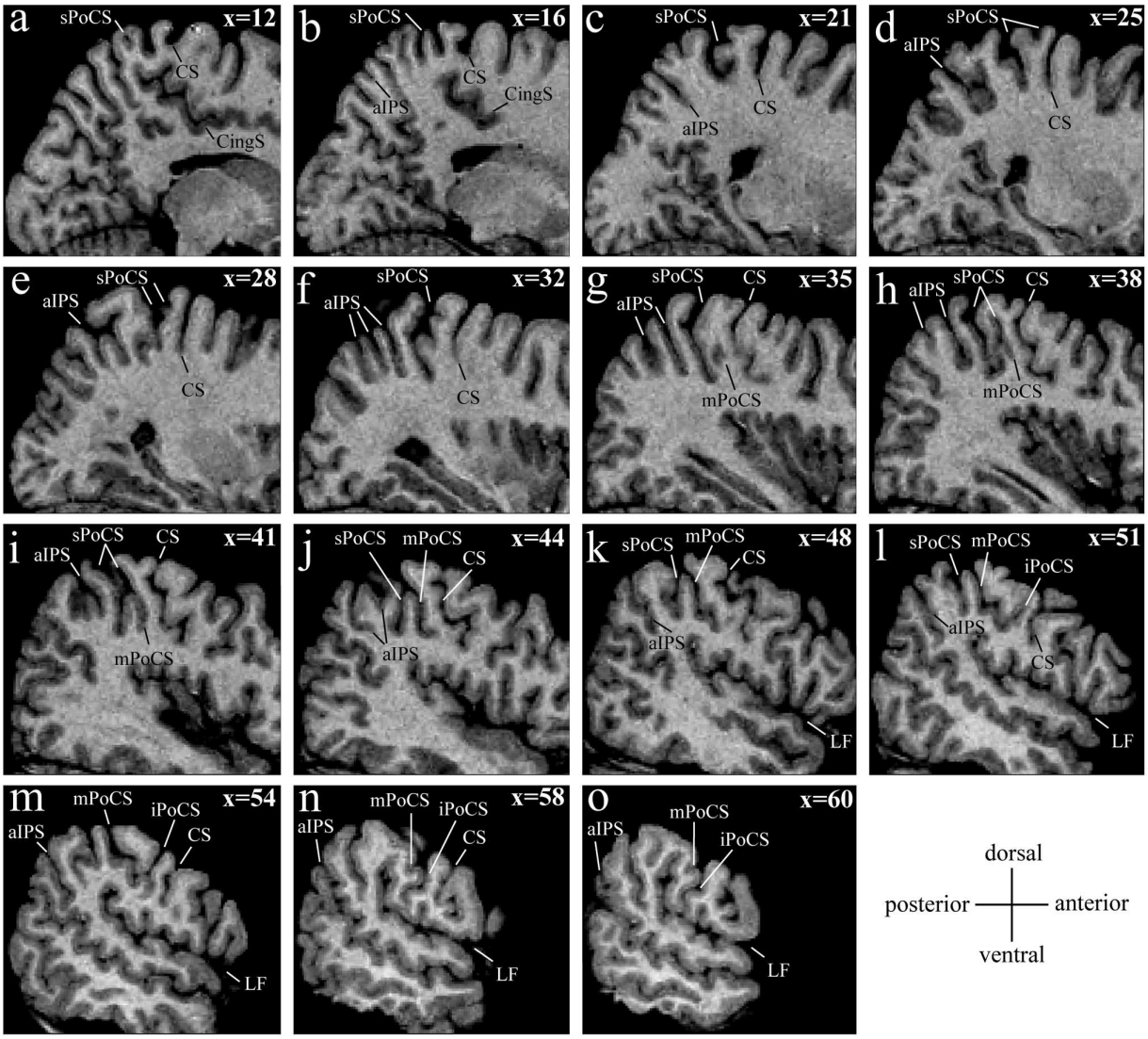

Figure 10. Sagittal sections from the right hemisphere of the MRI brain volume (case 2) with the sulci of interest identified. The level in the medio-lateral dimension (x coordinate) is given in millimetres for each section.

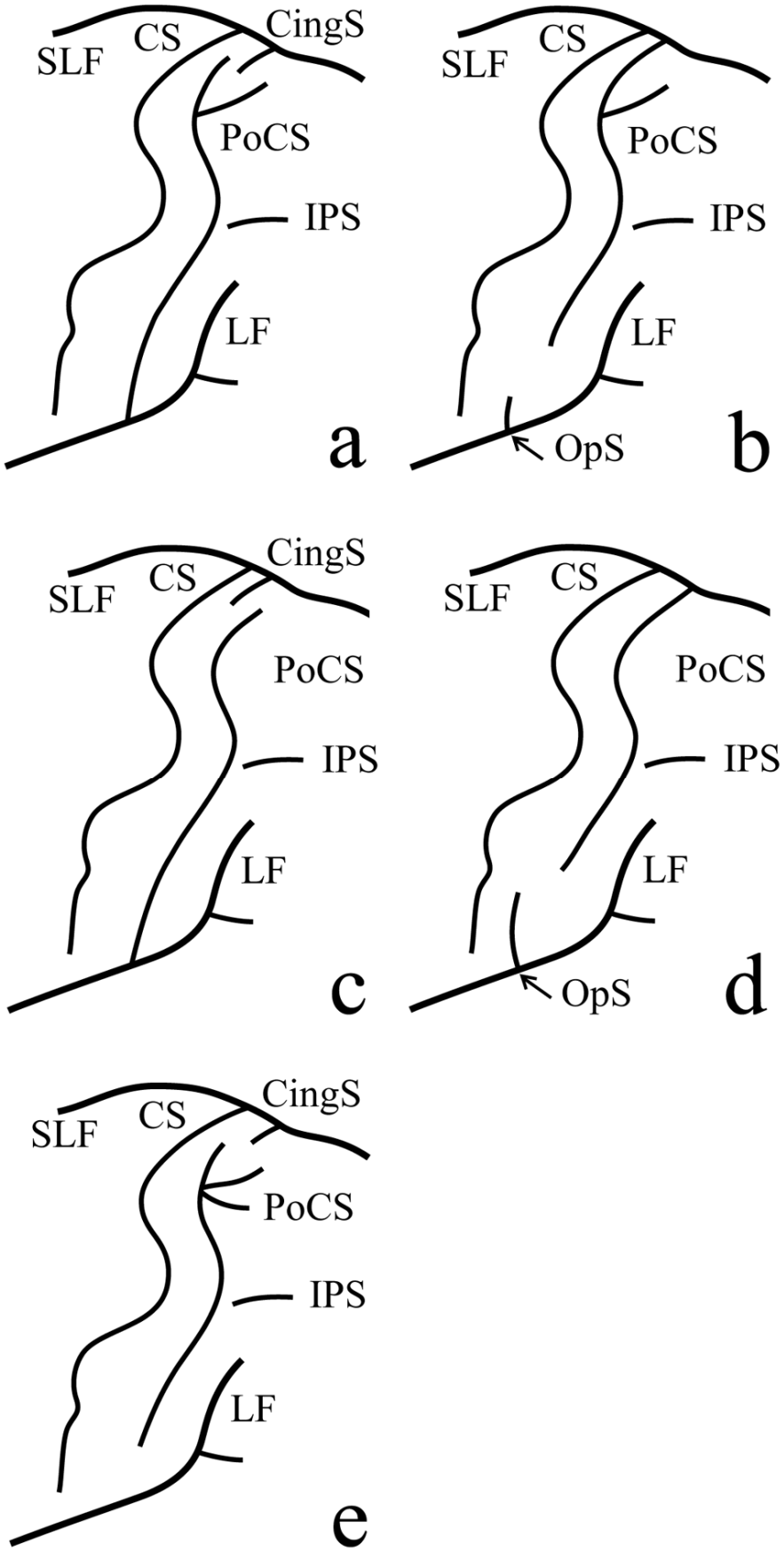
SLF
CS
CingS
PoCS
IPS
LF
a
SLF
CS
PoCS
IPS
LF
OpS
b
SLF
CS
CingS
PoCS
IPS
LF
c
SLF
CS
PoCS
IPS
LF
OpS
d
SLF
CS
CingS
PoCS
IPS
LF
e

Figure 11. Dorsal termination of the postcentral sulcus (PoCS). Superficial connection of the postcentral sulcus with the lateral fissure (LF) and the superior longitudinal fissure (SLF).

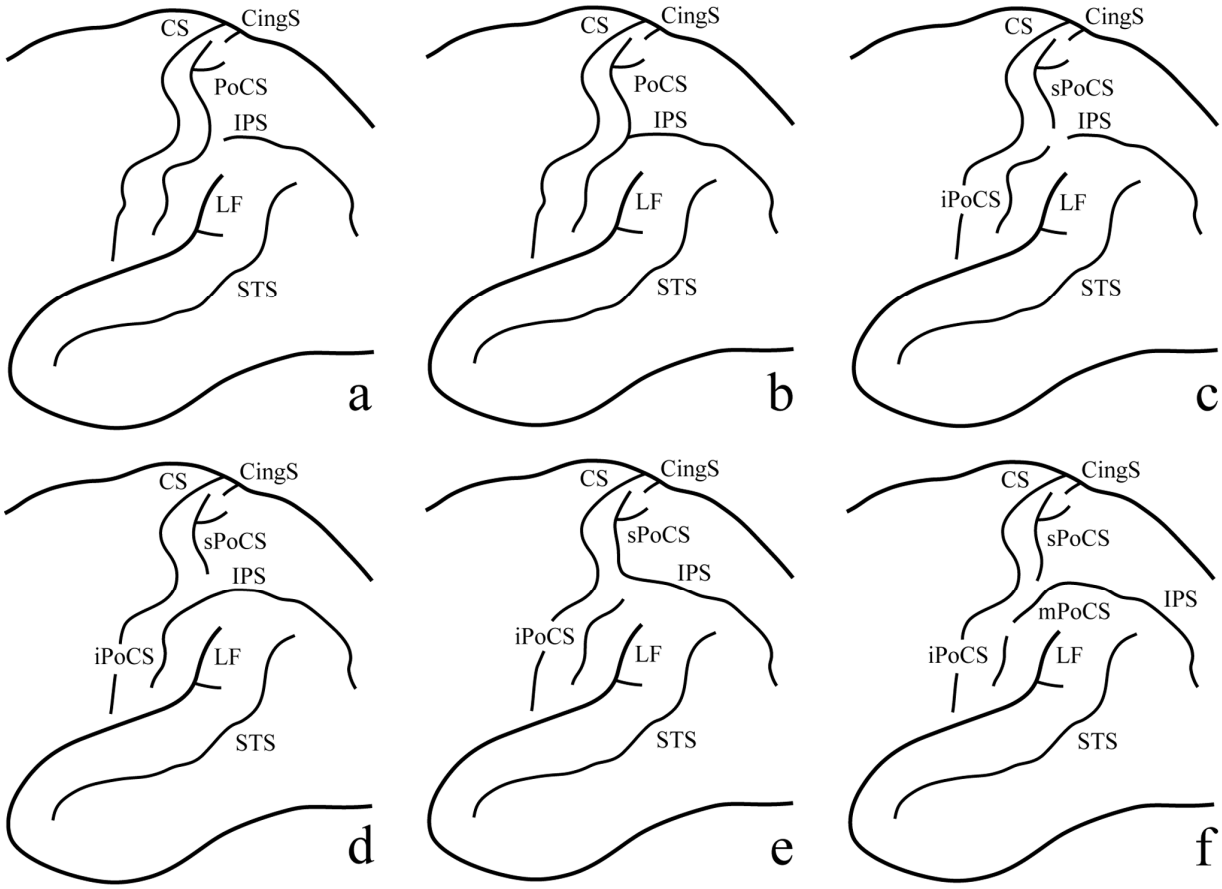

Figure 12. Patterns formed by the postcentral sulcal complex (PoCS) and the horizontal segment of the intraparietal sulcus (IPS) on the surface of the brain. In (**a**) a visible gyrus separates a continuous PoCS from IPS. IPS and PoCS do not merge. In (**b**) a gyrus between PoCS and IPS is submerged. IPS merges with the continuous PoCS on the surface of the brain only. In (**c**) a gyrus between sPoCS, iPoCS and IPS is visible on the surface of the brain. IPS and PoCS do not merge. In (**d**) a gyrus between sPoCS and IPS is visible on the surface of the brain. A gyrus between iPoCS and IPS is submerged. IPS merges with the iPoCS on the surface of the brain only. In (**e**) a gyrus between iPoCS and IPS is visible on the surface of the brain. A gyrus between sPoCS and IPS is submerged. IPS merges with the sPoCS on the surface of the brain only. In (**f**) a gyrus between mPoCS and IPS is submerged. mPoCS merges with IPS on the surface of the brain only.

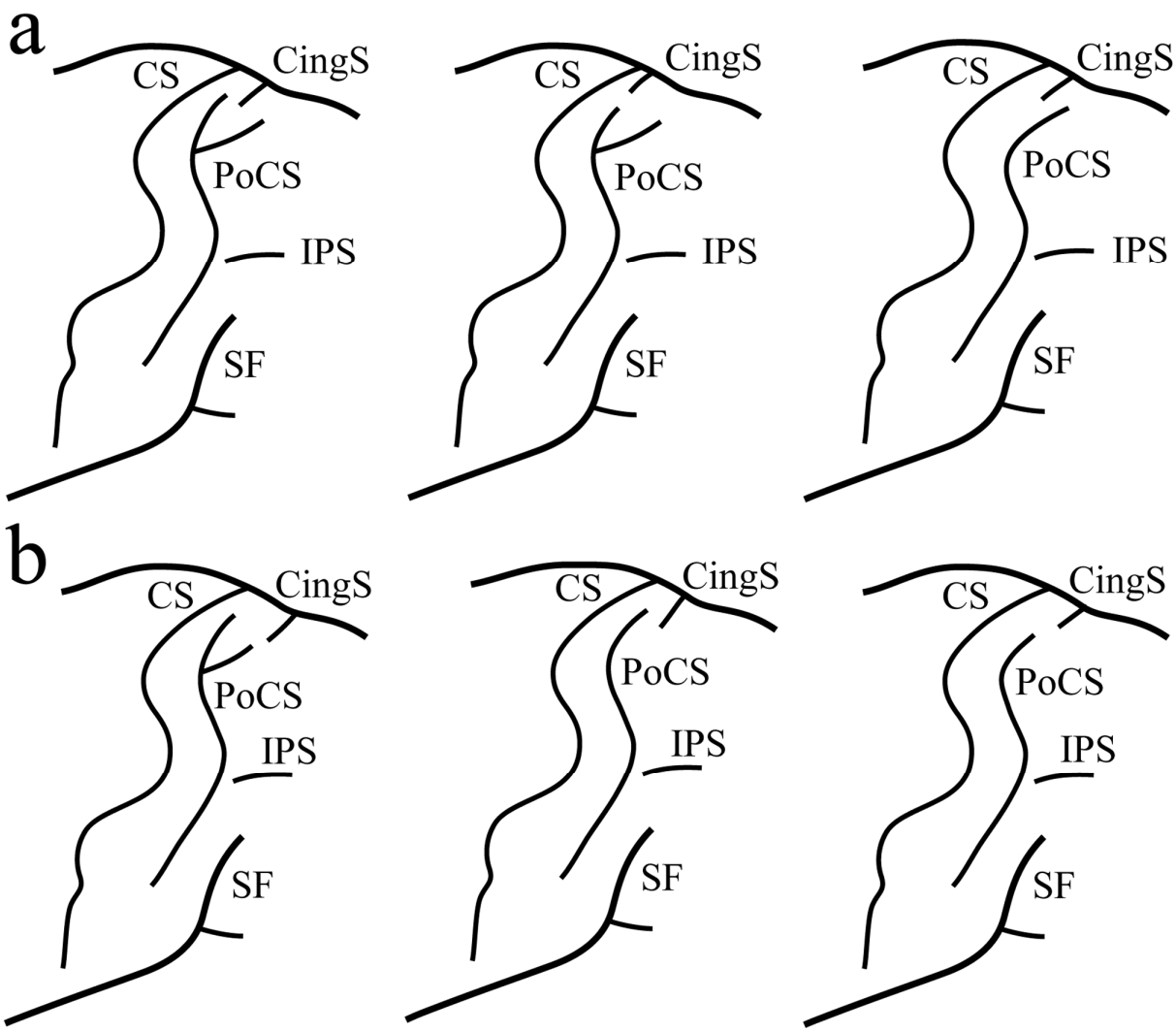

Figure 13. Patterns formed by the ascending branch of the cingulate sulcus (CingS) and the postcentral sulcus (PoCS). In (**a**) CingS terminates anterior to PoCS or inside a bifurcated dorsal end of PoCS. In (**b**) CingS terminates posterior to PoCS.

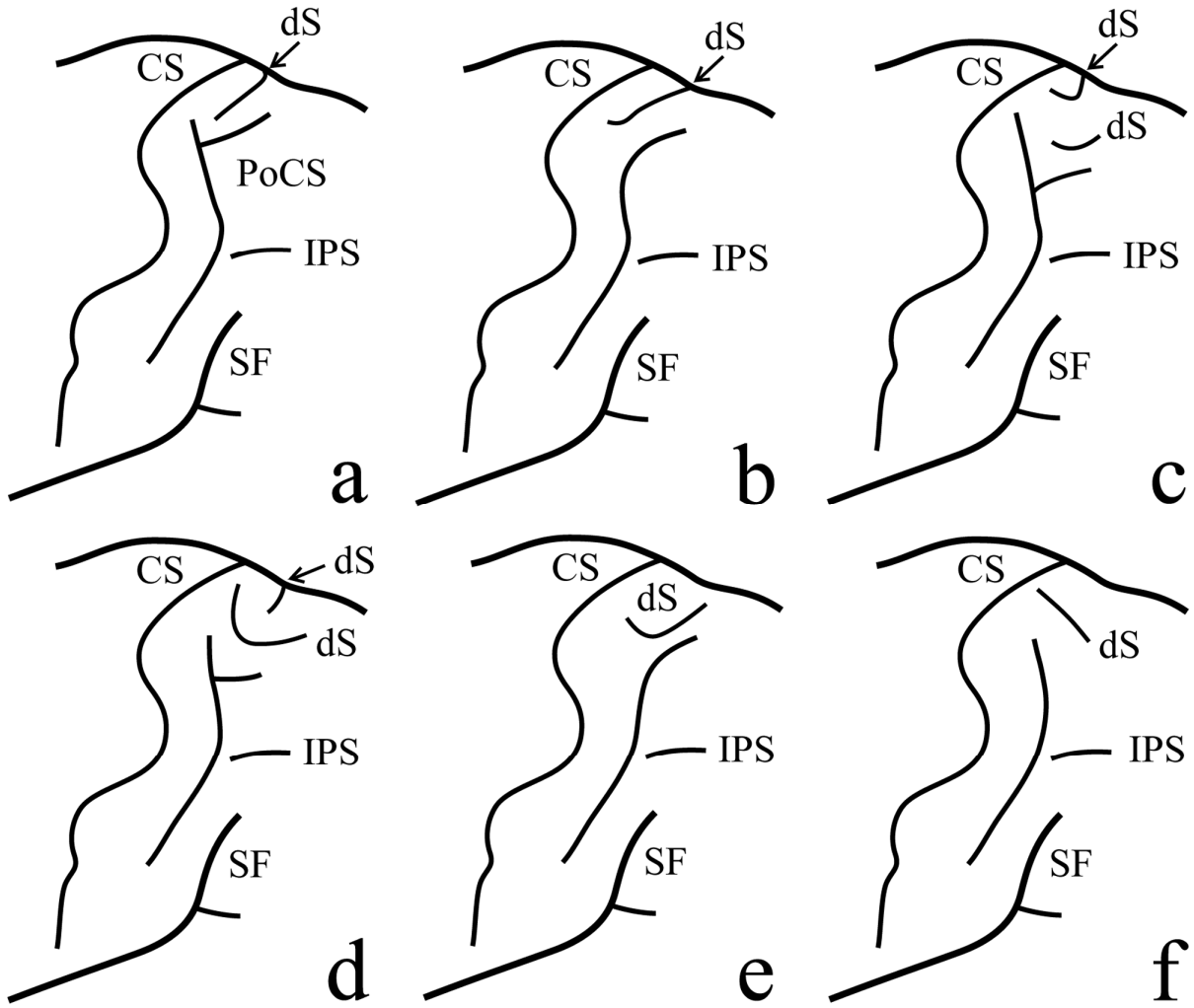

Figure 14. Sulci located dorsal (dS) to the postcentral sulcus (PoCS) on the lateral surface of the brain which cross (**a-d**) and do not cross (**c-f**) the superior margin of hemisphere. Ascending branch of the cingulate sulcus (CingS) is not visible on the lateral surface of the brain.

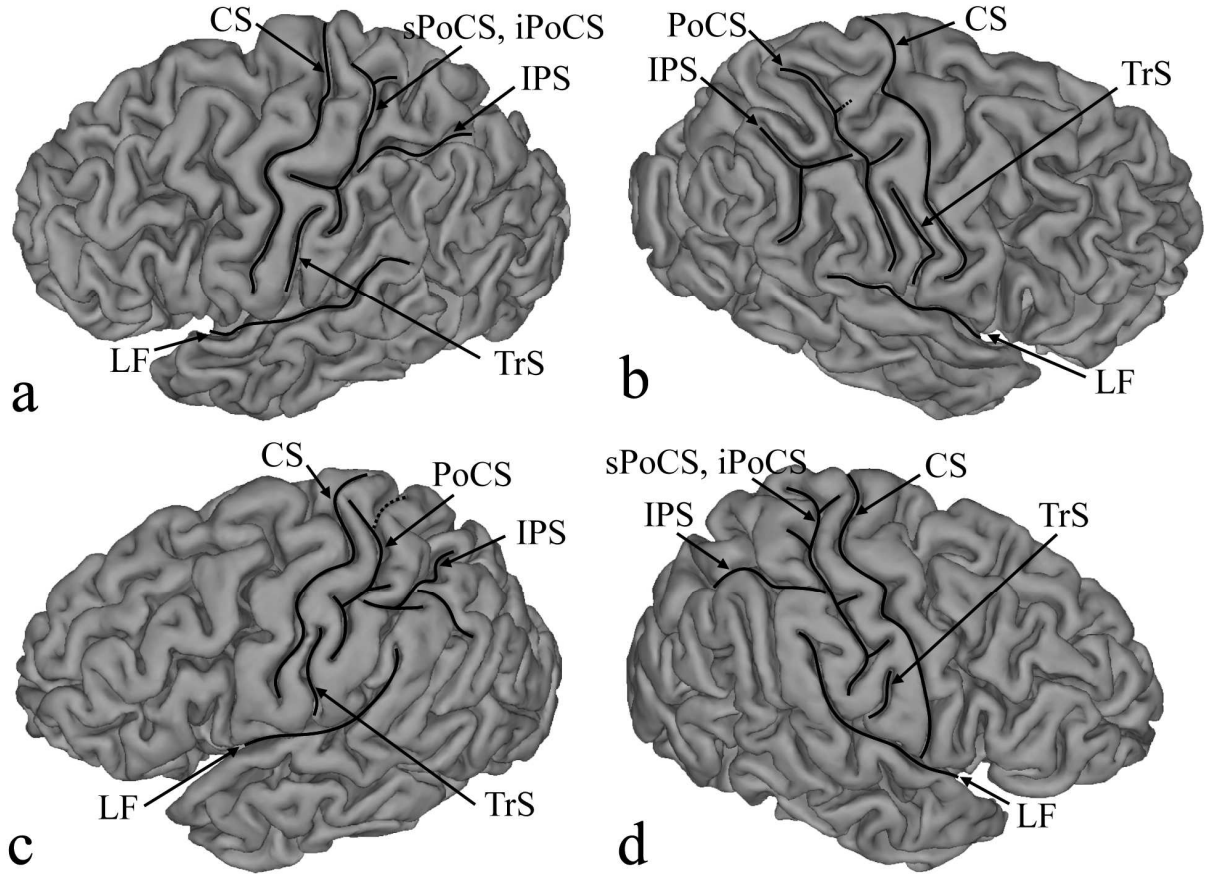

Figure 15. The transverse postcentral sulcus (TrS). In (**a**) the postcentral sulcus (PoCS) is divided into two segments, the superior and inferior postcentral sulci (sPoCS and iPoCS) by a submerged gyrus. The dorsal end of TrS is located at the 2nd submerged pli de passage. In (**b**) PoCS is continuous. The dorsal end of TrS is at the level of the 1st submerged pli de passage. In (**c**) PoCS is continuous. The dorsal end of TrS is located at the 2nd submerged pli de passage. In (**d**) PoCS is divided into 2 segments (sPoCS and iPoCS) by a submerged gyrus. The dorsal end of TrS is at the level of the 3rd submerged pli de passage.